The role of coupled DNRA-Anammox during nitrate removal in a highly saline lake

N. Valiente [a,b,*], F. Jirsa [c,d], T. Hein [e,f], W. Wanek [g], J. Prommer [g], P. Bonin [h], J.J. Gómez-Alday [b]

[a] Centre for Biogeochemistry in the Anthropocene, Department of Biosciences, Section for Aquatic Biology and Toxicology, University of Oslo, PO Box 1066, Blindern, 0316, Oslo, Norway
[b] Biotechnology and Natural Resources Section, Institute for Regional Development (IDR), University of Castilla–La Mancha (UCLM), Campus Universitario s/n, 02071 Albacete, Spain
[c] Institute of Inorganic Chemistry, Faculty of Chemistry, University of Vienna, Waehringer Strasse 42, 1090 Vienna, Austria
[d] Department of Zoology, University of Johannesburg, PO Box 524, Auckland Park, 2006 Johannesburg, South Africa.
[e] Institute of Hydrobiology and Aquatic Ecosystem Management, Department of Water, Atmosphere and Environment, University of Natural Resources and Life Sciences, Gregor-Mendel-Str. 33, 1180 Vienna, Austria
[f] WasserCluster Lunz – Inter-university Center for Aquatic Ecosystem Research, Lunz am See, Dr. Carl Kupelwieser Prom. 5, 3293 Lunz/See, Austria
[g] Division of Terrestrial Ecosystem Research, Centre of Microbiology and Environmental Systems Science, University of Vienna, Djerassiplatz 1, 1030 Vienna, Austria
[h] Aix-Marseille Université, CNRS, Université de Toulon, IRD, MIO UMR 110, 13288 Marseille, France

HIGHLIGHTS

- Denitrification, DNRA, and anammox coexist as nitrate removal processes.
- Contribution of each process is determined by oxygen and light conditions.
- DNRA and N_2O-denitrification prevail when oxygen and/or light are present.
- Anoxia and darkness promote nitrate reduction by combined DNRA-anammox.
- Coupled DNRA-anammox may be a relevant process in reducing atmospheric N_2O emissions.

GRAPHICAL ABSTRACT
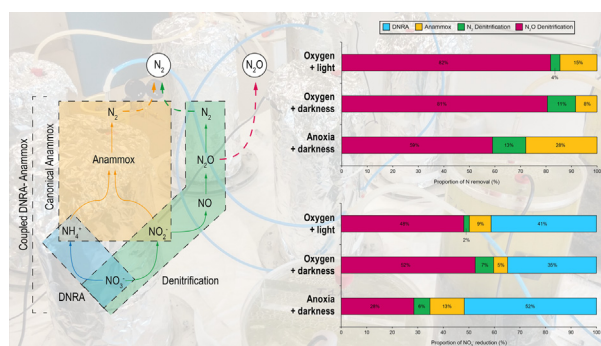
ARTICLE INFO

ABSTRACT

Nitrate (NO_3^-) removal from aquatic ecosystems involves several microbially mediated processes, including denitrification, dissimilatory nitrate reduction to ammonium (DNRA), and anaerobic ammonium oxidation (anammox), controlled by slight changes in environmental gradients. In addition, some of these processes (i.e. denitrification) may involve the production of undesirable compounds such as nitrous oxide (N_2O), an important greenhouse gas. Saline lakes are prone to the accumulation of anthropogenic contaminants, making them highly vulnerable environments to NO_3^- pollution. The aim of this paper was to investigate the effect of light and oxygen on the different NO_3^- removal pathways under highly saline conditions. For this purpose, mesocosm experiments were performed using lacustrine, undisturbed, organic-rich sediments from the Pétrola Lake (Spain), a highly saline waterbody subject to anthropogenic NO_3^- pollution. The revised ^{15}N-isotope pairing technique (^{15}N-IPT) was used to determine NO_3^- sink processes. Our results demonstrate for the first time the coexistence of denitrification, DNRA, and anammox processes in a highly saline lake, and how their contribution was determined by environmental conditions (oxygen and light). DNRA, and especially denitrification to N_2O, were the dominant nitrogen (N) removal pathways when oxygen and/or light were present (up to 82%). In contrast, anoxia and darkness promoted NO_3^- reduction by DNRA (52%), combined with N loss by anammox

---

* Corresponding author at: Centre for Biogeochemistry in the Anthropocene, Department of Biosciences, Section for Aquatic Biology and Toxicology, University of Oslo, PO Box 1066, Blindern, 0316, Oslo, Norway.
E-mail address: n.v.parra@ibv.uio.no (N. Valiente).

(28%). Our results highlight the role of coupled DNRA-anammox, which has not yet been investigated in lacustrine sediments. We conclude that anoxia and darkness favored DNRA and anammox processes over denitrification and therefore to restrict N_2O emissions to the atmosphere.

1. Introduction

Nitrogen (N) is an essential component of all living organisms and its availability controls the function of aquatic ecosystems. Microbial processes are controlling the Earth's N cycle for ~2.7 billion years. The microbial transformation of dissolved inorganic N to gaseous N forms is a pivotal sink that regulates the flux of N into the biosphere, being able to mitigate the effects of excessive anthropogenic inputs. Microbial processes in the inorganic N cycle have been widely studied in aquatic ecosystems, in both, water and sediments. Among inorganic N species, nitrate (NO_3^-) is a widespread compound, being responsible for water degradation due to excessive fertilizer use in agriculture (Spalding and Exner, 1993). NO_3^- accumulation can increase primary production in surface waters and, as a consequence, can trigger oxygen deficiency and promote eutrophication of surface waterbodies (Vitousek et al., 1997).

Denitrification is considered the primary process of NO_3^- removal in sediments, yielding N_2 as a main end product (hereafter referred to as N_2-denitrification), through a multi-step reduction process (Harrison et al., 2009; Fernandes et al., 2016; Kuypers et al., 2018). Nitrous oxide (N_2O) is an obligate intermediate of denitrification, which can also be its main end-product (hereafter referred to as N_2O-denitrification) (Trogler, 1999). Denitrification is strongly affected by oxygen availability. Despite that N_2O reductase (*nosZ*) activity has been considered to be inhibited at relatively low oxygen concentrations (0.25 mg/L) (Bonin and Gilewicz, 1991), recent studies showed the presence of *nosZ* gene or *nosZ* transcripts in potentially non-denitrifying genomes of aerobic genera like *Gemmatimonas* (Orellana et al., 2014; Yoon et al., 2016; Hallin et al., 2018). In addition to NO_3^- reduction by denitrifiers, heterotrophic bacteria in sediments may compete for NO_3^- in a second pathway leading to ammonium (NH_4^+), termed dissimilatory nitrate reduction to ammonium (DNRA). Denitrification and DNRA occur in parallel under anaerobic conditions, and the partitioning of the NO_3^- sink strength between these two processes appears to be the function of labile organic carbon to electron acceptor (i.e. NO_3^-) ratio (Bonin et al., 1999). Furthermore, under anaerobic conditions, anammox couples NH_4^+ oxidation to nitrite (NO_2^-) reduction to produce N_2 (Van de Graaf et al., 1995). The activity of anammox bacteria has been described in marine ecosystems (Thamdrup and Dalsgaard, 2002), including deep-sea hypersaline anoxic basins (Van der Wielen et al., 2005), and inland waters (Schubert et al., 2006; Abed et al., 2015; Roland et al., 2018). Anammox can be promoted by DNRA by supplying NH_4^+ (coupled DNRA-anammox) as described in the oxygen minimum zone of the Arabian Sea (Jensen et al., 2011).

The simultaneous occurrence of these pathways is of concern to the N budget and to greenhouse gas (N_2O) production. Indeed, reduction of NO_3^- to N_2, resulting from denitrification or anammox, leads to a rapid release of gaseous products from the ecosystem, whereas the alternative pathway (DNRA) keeps N in a readily available form and thus may cause persistent nutrient enrichment (Koike and Hattori, 1978). Thus, depending on the relative importance of these pathways, dissimilatory NO_3^- reduction either transforms inorganic N to gaseous (N_2 or N_2O) or reduced (NH_4^+) forms, causing it to be either retained or removed from the system. Furthermore, N_2O emissions have a profound effect on the environment, because N_2O is the main ozone-depleting agent and a powerful greenhouse gas (310 times more potent than carbon dioxide) (Ravishankara et al., 2009).

To quantify denitrification, DNRA, and anammox rates in sediments, core incubations have been frequently used by applying the ^{15}N isotope pairing technique (^{15}N-IPT) (Risgaard-Petersen et al., 2003; Roland et al., 2018). The ^{15}N-IPT was firstly applied on sediment cores to quantify N_2 production deriving from denitrification (Nielsen, 1992). Since then, many studies have focused on discriminating the relative contribution of inorganic N processes using ^{15}N-IPT, including DNRA and coupled DNRA-anammox (Risgaard-Petersen et al., 2003; Holtappels et al., 2011; Hsu and Kao, 2013; Deng et al., 2015; Robertson et al., 2019). Recently, an improved set of equations for ^{15}N-IPT have been published, allowing to estimate the contribution of N_2O production by N_2O-denitrification and the contribution of DNRA to NO_3^- reduction (Song et al., 2016; Salk et al., 2017). Prior to this revised methodology, coupled DNRA–anammox was indistinguishable from denitrification based on isotope tracer experiments (Francis et al., 2007). Hence, processes such as anammox have been traditionally underestimated, reinforcing the use of the new IPT approaches for a complete N balance estimation.

Among aquatic ecosystems, saline lakes are highly vulnerable to NO_3^- pollution. These ecosystems are mainly located in closed hydrological systems in arid and semi-arid regions, which, combined with low precipitation and high evaporation rates typical of arid climates, leads to the accumulation and biomagnification of many pollutants compared to freshwater systems (Williams, 2002). A large diversity and high potential activity of denitrifying bacteria have been previously observed in saline lakes (Kulp et al., 2007; Lipsewers et al., 2016), which was confirmed in denitrification studies at the field scale (Doi et al., 2004; Gómez-Alday et al., 2014; Valiente et al., 2018). In such ecosystems, variable redox conditions and the supply of organic matter (OM) and nutrients may lead to increased N_2O production by denitrification (Huttunen et al., 2003; Liu et al., 2015). In fact, N_2O reduction to N_2 seems to be a rate-limiting step during denitrification at extremely high salinities (Shapovalova et al., 2008). Anammox bacteria have also been detected in saline systems (Yang et al., 2012; Lipsewers et al., 2016), with a totally different community structure than described for freshwater lakes (Wang et al., 2015). So far, however, very little attention has been paid to the role of anammox processes in saline lakes, and we did not find any information on the role of coupled DNRA-anammox in these ecosystems.

As described above, oxygen plays a key role in favoring certain processes over others. In addition, light availability can affect the balance between NO_3^- removal pathways, as light enhances primary production and the production of dissolved oxygen. This study explores the different ways in which NO_3^- is removed under highly saline conditions, as well as how light and oxygen levels determine the importance of certain sink processes over others. For this purpose, we incubated lacustrine sediments from a eutrophic saline lake (Pétrola Lake, Spain) and applied the revised ^{15}N-IPT approach to quantify inorganic N-cycling rates. We tested the hypothesis that oxygen availability and light exposure of the water column promote denitrification over DNRA and anammox in the sediment-water interface. Taken together, these findings not only improve our knowledge of the mass balance of N pollutants in saline lakes, but also of how their removal depends on environmental conditions (e.g. light, oxygen) and may impact the global scale by producing undesired by-products (e.g. N_2O release).

2. Materials and methods

2.1. Study site

Samples were collected from Pétrola Lake (38° 50' 14" N, 1° 33' 40" W), 35 km southwest of Albacete, Spain. Pétrola Lake (1.76 km²) is the main wetland in the endorheic Pétrola–Corral-Rubio–La Higuera

Saline Complex, located in a zone vulnerable to eutrophication, though fertilizer use is restricted (Order 2011/7/2 CMA). For a detailed description of the study area, see Valiente et al. (2017). Despite that the Pétrola endorheic basin was declared vulnerable to NO_3^- pollution by the Regional Government of Castilla-La Mancha in 1998, it still receives a continuous supply of inorganic N originating from inorganic synthetic fertilizers (Valiente et al., 2018). As a result, eutrophication of the water layer occurs, leading to the dominance of phytoplankton, reducing light penetration, and promoting bottom-water oxygen depletion because of bacterial decomposition. The dominant phytoplankton includes diatoms (*Amphora* spp., *Nitzschia* spp.), cyanobacteria (*Oscillatoria* spp., *Phormidium* spp.), and green algae (*Chlamydomonas* spp., *Tetraselmis* spp.) (information from Confederación Hidrográfica del Segura, Spain, unpublished data).

The field survey was conducted in July 2015. The sampling site was approximately 50 cm deep, located close to the lake's depocenter, without any direct input of polluted freshwater streams or wastewaters. We therefore consider it representative of the natural conditions of the lake. To evaluate initial in situ natural conditions (NC), surface water samples were collected, filtered through 0.45 μm pore size nylon filters and stored at 4 °C in darkness prior to further analyses. Furthermore, sediment cores ($n = 3$) were taken from the upper 20 cm lacustrine sediment using acrylic coring tubes (5 cm inner diameter, 20 cm length). The coring tubes were capped at the top and the bottom with silicone rubber stoppers, cooled, and transported to the laboratory. Once there, the top 5 cm of each core was sliced and used for inorganic N-species extraction. Afterwards, these slices were then frozen at -20 °C for further analyses.

Mesocosm preparation for core incubations was adapted from previous works (Welti et al., 2012), except for the use of a feeding water reservoir. For this purpose, acrylic mesocosms (40 cm in length, 20 cm in diameter, containing a total volume of 12.6 L) were used for sampling and incubation to guarantee minimal disturbance of the sediment during sampling ($n = 9$). The mesocosm tubes were acid-prewashed and then drilled into the sediment down to approximately 20 cm depth. Then, mesocosms were filled with 2 L of lake water to maintain sediment saturation during transport. Additional lake water was collected from the sampling point and stored at 4 °C to fill the mesocosms in the lab. Black plastic sheets were used to cover the mesocosms to prevent light penetration during transport.

2.2. Sediment incubations

In the lab, each mesocosm was filled with lake water, reaching a water volume of approximately 6.3 L, and bubbled with either air (oxic treatment) or argon (anoxic treatment). Each mesocosm was tightly sealed. The upper part consisted of a screw-on lid with two holes (2 cm inner diameter) and a rubber stopper placed in each hole. For sample collection, a Teflon tube (4 mm inner diameter) was installed through each rubber cap. The tube inlet was placed 1 cm over the sediment surface, whereas the tube outlet was closed to the atmosphere with a three-way valve. In order to maintain water circulation inside each mesocosm, a small aquarium pump was installed in the inner wall to prevent stagnation. Mesocosms were placed in a temperature-controlled room to mimic water temperature conditions in summer months (25 °C; Valiente et al., 2018), with no exposure to direct sunlight.

Three different treatments were studied in triplicate. Treatment 1 (OL; oxygen + light) mimicked field conditions by means of atmospheric air bubbling, to provide oxygen, and normal dark-light cycles (~ 14 h of light per day; no additional light source was used). Mesocosms of treatment 1 ($n = 3$) were placed close to the room window. OL is henceforth considered as control. For treatment 2 (OD; oxygen + darkness), oxic conditions in the water column were preserved via atmospheric air bubbling. However, each mesocosm was covered with aluminum foil to protect it from light. Finally, treatment 3 (AD;

anoxia + darkness) maintained anoxic conditions by bubbling with a mixture of N_2 and 1% Ar, and mesocosms were shielded from light. The bubbling fluxes applied in the experiments were established based on the maximum solubility values of N_2 (Hamme and Emerson, 2004) and N_2O (Weiss and Price, 1980) in seawater, using a salinity value of 50 g/L, similar to the one previously reported in Pétrola Lake (Valiente et al., 2018). Mesocosms were equilibrated in the laboratory until constant $N-NO_3^-$ and $N-NO_2^-$ concentrations in the water column were reached. During the stabilization period (stage S0), physicochemical parameters, and inorganic N-species were monitored at 12 h intervals, starting 12 h after collection of the sediment cores (time -36), and finishing 48 h after field sampling (time 0) with $N-NO_3^-$ concentration constantly below the limit of detection (LOD, <0.05 μM).

In order to apply the ^{15}N-IPT approach to quantify NO_3^- transformation processes in the mesocosms, ^{15}N-labeled NO_3^- ($K^{15}NO_3$, 98 atom% at ^{15}N) was added once mesocosm stabilization was reached (time 0). This involved spiking with 250 μmol of $^{15}NO_3$, reaching a water column concentration of about 40 μM $N-NO_3^-$. After labeled NO_3^- addition (stage S1), the sampling frequency and incubation times were calculated following the NICE handbook (Dalsgaard et al., 2000). Thus, 30 min intervals were adopted as the initial sampling rate: this was calculated as the optimal time to enable denitrification to reach 90% of its steady state value, assuming in the oxic treatment a sediment penetration depth of oxygen of 1 mm based on previous works (Valiente et al., 2017). The frequency of sampling decreased at stage S2 (from time 24 h until the end of the experiment) with respect to stage S1 (from time 0 to 24 h). In each mesocosm, water samples (20 mL) were taken from the water column for inorganic N-species and N-isotope analysis ($N-NO_3^-$, $N-NH_4^+$, N_2, and N_2O) at times 0, 0.5, 1, 1.5, 2, 2.5, 3, 4, 5, 6, 8, 10, 12, 15, 18, 24, 30, 36, 48, 60, and 72 h with a 50 mL syringe. Moreover, water samples (10 mL) for physico-chemical analyses, dissolved organic carbon (DOC) and dissolved bound nitrogen (DNb) determination were collected at times 0.5, 2, 4, 8, 12, 24, 48, and 72 h from each collection Teflon tube using a 50 mL syringe. At the end of the incubations, sediment samples were obtained from the upper 5 cm of each mesocosm, homogenized using a spatula, and used fresh for chemical analyses. Sediment samples were frozen (-20 °C) before further analyses.

2.3. Physico-chemical analyses

Physico-chemical parameters measured included temperature, pH, electrical conductivity (EC), total dissolved solids (TDS, used for salinity estimation), redox potential (Eh), and dissolved oxygen (DO). These parameters were determined directly in the surface water from site 2651 using a HQ40d Portable Multi-Parameter Meter (Hach Company, USA). During sediment incubations, physico-chemical parameters were measured in the collected water samples. Collected water samples were immediately filtered through a 0.45 μm nylon Millipore® filter. Inorganic N-species were determined directly after collection at the Institute for Regional Development (University of Castilla-La Mancha, Spain). Determination of NO_2^- and NO_3^- concentration was achieved by UV-VIS spectrophotometry via the modified Griess reaction assay as described by García-Robledo et al. (2014). NH_4^+ concentrations were quantified by UV-VIS spectrophotometry using the modified indophenol method, as described by Hood-Nowotny et al. (2010). Dissolved inorganic nitrogen (DIN) was calculated by summing up the concentrations of $N-NO_2^-$, $N-NO_3^-$, and $N-NH_4^+$. DOC and DNb measurements were performed using a Shimadzu TOC-V Analyzer with a total N measurement unit (TNM-1) at the Institute of Inorganic Chemistry of the University of Vienna, Austria. For DOC, samples were acidified to pH ≈ 2 with 2 M HCl followed by 5 min purging to remove all dissolved inorganic carbon. Dissolved organic nitrogen (DON) concentrations were estimated by subtracting DIN from the measured DNb, considering DNb as the sum of dissolved N species (organic and inorganic N) excluding gaseous N forms.

Sedimentary N-NO$_3^-$ (S-N-NO$_3^-$), N-NH$_4^+$ (S-N-NH$_4^+$), and N-NO$_2^-$ (S-N-NO$_2^-$) were determined after extraction of fresh sediments with 1 M KCl (1:7.5 (w:v)) following Hood-Nowotny et al. (2010). Frozen sediment samples were lyophilized for 48 h, followed by homogenization in a porcelain mortar and sieving through a 1 mm steel sieve. Organic matter (OM) content in dried sediment samples was determined as loss of ignition (LOI) by combusting dried sediments for 2 h at 550 °C at the Institute of Inorganic Chemistry of the University of Vienna, as described by Nelson and Sommers (2018).

2.4. Isotope composition of N species

The isotopic composition of N-NH$_4^+$ in the water column was determined by a microdiffusion method using MgO and acid traps (Brooks et al., 1989; Lachouani et al., 2010). The isotopic composition of N-NO$_3^-$ was measured in the previously microdiffused extracts by a reduction-microdiffusion method after conversion by Devarda's alloy to N-NH$_4^+$ (Prommer et al., 2014). The recovery efficiency of the conversion was ≥95% (Sørensen and Jensen, 1991; Mulvaney et al., 1997). The filter discs from the acid traps were dried and analyzed for N content and at.% ^{15}N by elemental analyzer-isotope ratio mass spectrometry (EA-IRMS) using an elemental analyzer (EA 1110, CE Instruments) connected via a ConFlo III interface (Thermo Fisher) to a DELTA^{plus} IRMS (Finnigan MAT) in the SILVER Lab (University of Vienna).

To measure the isotopic composition of N$_2$ and N$_2$O, water samples were collected by 60-mL plastic syringes and transferred to gas tight vials containing 1 mL 100 mM HgCl$_2$ to halt biological reactions. Each vial was completely filled with water sample avoiding any gas headspace. All vials were stored and shipped to the Mediterranean Institute of Oceanography (Aix-Marseille Université, France) for the analysis of N$_2$ (^{29}N$_2$ and ^{30}N$_2$) and N$_2$O isotopic species concentrations (^{44}N$_2$O, ^{45}N$_2$O, and ^{46}N$_2$O) using GC–MS (Stevens et al., 1993). Dissolved N$_2$ and N$_2$O were extracted from the samples in the vials by introducing a 6 mL He headspace while simultaneously removing 6 mL of water sample. Sample injection was performed using a modified head-space autosampler (TriPlus 300, Thermo Fisher) that involves gas-equilibration at 65 °C for 6 min whilst shaking vigorously, so that more than 98% of the N$_2$ and N$_2$O equilibrium concentration was attained (Weiss, 1970). GC–MS analysis was performed using an Interscience Compact GC system equipped with AS9-HC and AG9-HCT columns. N$_2$ was measured at $m/z = 28$, 29 and 30 corresponding to ^{28}N$_2$, ^{29}N$_2$ and ^{30}N$_2$, respectively. Ar was used as an internal standard (Minjeaud et al., 2009; Fernandes et al., 2012; Welti et al., 2012). O$_2$ and Ar were measured at m/z = 32 and m/z = 40, respectively. Finally, isotopic mass balance calculations were performed using discrete time points compared to the originally added amount of ^{15}NO$_3$. Starting from the initial amount spiked (250 μmol K^{15}NO$_3$), N concentrations and atom percent enrichments were used to calculate the percentage of ^{15}N recovery in specific N forms and overall.

2.5. Denitrification, DNRA, and anammox activity measurements

For ^{15}N-IPT modeling, the revised ^{15}N-IPT calculation procedure (Salk et al., 2017) was applied. A detailed description of parameters and equations is provided in the Supporting Information (Table S1). For this purpose, our incubations were assumed to be intact core incubations. The probabilities of NO$_3^-$ reduction via denitrification, DNRA, and anammox were assumed to be equal (Song et al., 2016). Genuine N$_2$ production via denitrification (D_{14}) and anammox (A_{14}), as well as N$_2$O production via denitrification, were calculated for each time step. Production rates were calculated according to Salk et al. (2017) for each time point after the addition of the labeled ^{15}NO$_3^-$. Non-linear increments in the ^{15}N content were taken into account by calculating the N production rates (i.e. ^{15}NH$_4^+$, ^{29}N$_2$, ^{30}N$_2$, ^{45}N$_2$O, ^{46}N$_2$O) from the slope of the initial time point and each specific time point rather than

a slope of all time points. Thus, a total of 20 rates of each process were calculated for each mesocosm. Ratios of ^{14}NO$_3^-$:^{15}NO$_3^-$ (r_{14}) and ^{14}NH$_4^+$:^{15}NH$_4^+$ (r_{14a}) were calculated and used as base parameters for activity calculations. The applied methodology allowed distinguishing between N$_2$ production via coupled DNRA-anammox and via canonical anammox (using non-DNRA-derived NH$_4^+$). DNRA rates were calculated using the production of ^{15}NH$_4^+$, and of ^{30}N$_2$ for anammox, over time. However, this model cannot discriminate between ^{15}NO$_3^-$ assimilation and subsequent remineralization of OM to ^{15}NH$_4^+$, and DNRA. Thus, the DNRA rate may include both processes. The sum of N$_2$ production by denitrification and anammox, together with N$_2$O production via denitrification, is designated as 'Total N loss'. The 'Total NO$_3^-$ reduction' adds the DNRA rate to the previous estimate. In addition to this isotope-based approach, specific fluorescence in situ hybridization (FISH) probes were used to detect microorganisms capable of performing such processes (Table S2). Methodological details about FISH can be found in the Supporting Information.

2.6. Statistical analysis

Changes in chemistry and rates of N-loss processes over time as well as at the end of the incubation were assessed using one-way analysis of variance (ANOVA), followed by the Tukey's post hoc test (homogeneous variances) or by the Games-Howell post hoc test (heterogeneous variances). To assess differences in the hydrochemical conditions between initial ($n = 1$) and final conditions ($n = 9$), one-sample two-tailed t-tests were used. Results of statistical tests were considered to be significant at a confidence level of 95% ($\alpha = 0.05$). All tests were performed using SPSS-IBM Statistics software.

3. Results

3.1. Differences between treatments in chemical parameters

Differences between initial (NC$_{-48}$; time -48 h) and final conditions (OL$_{72}$, OD$_{72}$, and AD$_{72}$; time 72 h) were assessed for the three treatment groups (Table 1). For inorganic N-species in the water column, the final N-NO$_3^-$ and N-NO$_2^-$ concentrations were below LOD. N-NH$_4^+$ concentrations increased significantly (t-test, $p < 0.05$) between NC$_{-48}$ and final conditions in the treatments OL$_{72}$ ($t_{(2)} =$ 8.33), OD$_{72}$ ($t_{(2)} = 17.89$) and AD$_{72}$ ($t_{(2)} = 19.23$). Furthermore, there was a significant effect of light on the N-NH$_4^+$ concentration ($F_{(2,6)} =$ 15.98). Tukey's post hoc tests indicated that the final N-NH$_4^+$ concentration in OL$_{72}$ (139 ± 15.7 μmol/L) was significantly lower than in OD$_{72}$ (175 ± 10.9 μmol/L) and AD$_{72}$ (198 ± 12.2 μmol/L). N$_2$ and N$_2$O final concentrations (time 72 h) did not show significant differences between treatments ($F_{(2,6)}$ of 0.55 and 0.54, respectively).

DOC concentrations increased significantly between NC$_{-48}$ and final conditions in OL$_{72}$ ($t_{(2)} = 6.30$) and OD$_{72}$ ($t_{(2)} = 9.89$), but not in AD$_{72}$ ($t_{(2)} = 3.79$). Between treatments, there were no significant differences in DOC ($F_{(2,6)} = 0.91$). DNb and DON concentrations did not change over time ($p > 0.05$), and did not differ between treatments ($F_{(2,6)}$ of 1.28 and 0.95, respectively). The contribution of DON to DNb (DON:DNb) decreased significantly between NC$_{-48}$ and final conditions in all treatments (OL$_{72}$, $t_{(2)} = -26.4$; OD$_{72}$, $t_{(2)} = -6.89$; AD$_{72}$, $t_{(2)} = -8.28$), and differed between treatments ($F_{(2,6)} = 5.31$). Between initial (8.70, NC$_{-48}$) and final conditions, values decreased significantly for pH (OL$_{72}$, $t_{(2)} = -17.14$; OD$_{72}$, $t_{(2)} = -10.26$; AD$_{72}$, $t_{(2)} = -6.43$) and Eh (OL$_{72}$, $t_{(2)} = -7.81$; OD$_{72}$, $t_{(2)} = -8.88$; AD$_{72}$, $t_{(2)} = -5.15$) in the three treatments. Between treatments, only pH showed significant differences ($F_{(2,6)} = 5.37$). At the end of the experiment, the highest mean pH values were found in the oxic treatments, being slightly higher than the mean pH measured in the AD treatment (Table 1). Salinity, estimated as TDS values, was around the hypersaline limit (50 g/L), with values ranging from 45.1 g/L (NC$_{-48}$) to 50.1 g/L (AD$_{72}$). In the sediment samples, LOI ($F_{(3,8)} = 0.50$) and S-N-

Table 1

Mean values (±SD) of physico-chemical parameters in water and sediment for the experiments at the beginning and at the end of incubations.

Treatment	Conditions water column	pH	Eh (mV)	DO (mg/L)	EC (mS/cm)	TDS (g/L)	DOC (mmol/L)	DNb (mmol/L)	DON (mmol/L)
NC_{-48} (*)	Natural conditions (lake)	8.70	+135.1	4.26	72.1	45.1	16.3	1.07	1.00
OL_{72} ($n = 3$)	Aeration and light	7.89 ± 0.08	-105.7 ± 28.1	6.46 ± 0.26	75.9 ± 3.90	45.5 ± 3.30	27.0 ± 2.9	1.12 ± 0.17	0.98 ± 0.16
OD_{72} ($n = 3$)	Aeration and darkness	7.93 ± 0.13	-114.3 ± 41.0	6.40 ± 0.73	76.8 ± 0.86	47.1 ± 0.56	31.3 ± 2.6	1.30 ± 0.15	1.12 ± 0.15
AD_{72} ($n = 3$)	Anoxia and darkness	7.40 ± 0.35	-370.7 ± 7.51	0.08 ± 0.02	80.9 ± 0.91	50.1 ± 0.80	28.7 ± 5.7	1.21 ± 0.08	1.01 ± 0.09

Treatment	DON:DNb (%)	$N-NO_3$ (μmol/L)	$N-NH_4$ (μmol/L)	$N-NO_2$ (μmol/L)	N_2 (mmol/L)	N_2O (mmol/L)	LOI (%)	$S-N-NO_3$ (μmol kg^{-1})	$S-N-NH_4$ (mmol kg^{-1})	$S-N-NO_2$ (μmol kg^{-1})
NC_{-48} (*)	93.2	9.25	63.1	BLD	n.a.	n.a.	8.50 ± 2.06	17.1 ± 2.78	1.28 ± 0.37	BLD
OL_{72} ($n = 3$)	87.5 ± 0.5	BLD	139 ± 15.7	BLD	6.07 ± 0.28	0.52 ± 0.05	8.84 ± 1.56	68.4 ± 13.4	0.60 ± 0.27	BLD
OD_{72} ($n = 3$)	86.4 ± 1.7	BLD	175 ± 10.9	BLD	5.88 ± 0.02	2.28 ± 2.69	8.51 ± 1.46	64.6 ± 24.4	1.22 ± 0.76	BLD
AD_{72} ($n = 3$)	83.5 ± 2.0	BLD	198 ± 12.2	BLD	6.27 ± 0.74	2.23 ± 3.09	9.90 ± 1.31	73.2 ± 16.0	1.83 ± 0.27	BLD

(*) At NC_{-48}: $n = 1$ in water samples for determination of all the chemical parameters, as it corresponds to the in situ conditions in the lake; $n = 3$ in sediment samples (LOI, $S-N-NO_3$, $S-N-NH_4^+$, and $S-N-NO_2$). Subscripts indicate time of sampling: initial (-48 h) or final (72 h). Eh: redox potential. DO: dissolved oxygen. EC: electrical conductivity. TDS: total dissolved solids. DOC: dissolved organic carbon. DNb: dissolved bound nitrogen. DON: dissolved organic nitrogen. LOI: loss of ignition. BLD: below limit of detection. n.a.: not available.

NH_4^+ ($F_{(3,8)} = 3.54$) did not differ ($p > 0.05$) between NC_{-48} and final conditions or between treatments. Significant differences were found in $S-N-NO_3^-$ concentrations over time ($F_{(3,8)} = 7.81$), but not between treatments.

3.2. Hydrochemical evolution

The complete evolution of N-species over time is included in the Supporting Information (Fig. S1). During the stabilization period (S0), $N-NO_3^-$ was absent from the water column. Immediately after tracer addition (time 0), $N-NO_3^-$ increased markedly and then gradually decreased (stage S1), declining fastest in the AD treatment (anoxia and darkness). During the final stage (S2), $N-NO_3^-$ remained below LOD. This trend was also observed in Fig. 1, where ^{15}N evolution is shown over time. There, $^{15}NO_3^-$ reached the maximum concentrations at 6 h (OL treatment), 12 h (OD treatment), and 1 h (AD treatment), and was completely removed from the water column within the first 36 h (OL and OD), or even faster (12 h, AD treatment). $N-NO_2^-$ peaked during stage S1, paralleling the decrease in $N-NO_3^-$. Subsequently, $N-NO_2^-$ decreased faster in treatment AD than in the oxic treatments (OL and OD), as observed for $N-NO_3^-$, and remained below LOD. In contrast, $N-NH_4^+$ in the water column increased over time in all treatments. The concentration moderately increased during the stabilization period (S0) in all treatments (Fig. S1). From the addition of the labeled NO_3^- onwards, $N-NH_4^+$ increased (with small oscillations) coupled with a constant increase in $^{15}NH_4^+$ (Fig. 1) up to 18 h of incubation. This increase was more pronounced in the AD than in the OD and OL treatments. From 24 h to the end of the incubation, $N-NH_4^+$ concentration increased, whereas $^{15}NH_4^+$ tended to stabilize. Concentrations of N_2 were measured starting with the addition of the $^{15}NO_3^-$. In general, Fig. S1 showed a stable concentration of N_2 over time (above 6 mmol/L), with small peaks in the first 12 h of incubation (positive for the OL and AD treatments, negative for the OD treatment). By comparing these data with $^{15}N_2$ evolution data (Fig. 1), small variations in both $^{29}N_2$ and $^{30}N_2$ were observed after the tracer addition, where the sharp increase of N_2 in the OD treatment at 48 h coincided with an abrupt rise in $^{30}N_2$. Considering N_2O evolution, a different pattern was observed than that described for N_2. An increasing trend was observed in $N-N_2O$ in all three treatments. $^{45}N_2O$ accumulated towards the end of the incubations, especially in treatments OD and AD, with total N_2O concentrations above 2.0 mmol/L. Finally, the solubility of N_2O at 50 g/L of salinity and 25 °C was 14.25 mmol/L, whereas the solubility for N_2 at the same conditions was significantly lower (0.43 mmol/L). Therefore, N_2 oversaturation was observed in the water column.

In addition, the ^{15}N mass balance was calculated to detect whether gas bubbling (atmospheric air or argon to maintain aerobic or anoxic states) and differences in solubility may strip $^{29}N_2$ and $^{30}N_2$ faster than $^{45}N_2O$ and $^{46}N_2O$ (Supporting Information, Fig. S2). Mean ^{15}N recoveries were 92% for OL (from 79 to 108%), 94% for OD (from 67 to 125%), and 93% for AD (from 73 to 126%). Mass losses of 6-8% based on whole-system ^{15}N recoveries are very small and may derive mainly from the accumulation of errors in the ^{15}N measurements (concentrations and at.%^{15}N enrichments) of 5 dissolved and gaseous N pools. Therefore, we consider that there were no significant N losses deriving from gas bubbling.

Finally, Fig. S3 (Supporting Information) shows the whole evolution of physico-chemical parameters during the incubations. The evolution of DOC and DON in the water column showed stable concentrations during the stabilization period (S0), followed by a sharp increase in S1 after tracer addition. After that, DOC tended to decrease towards the end of the experiment, while DON had a tendency to stabilize. Moreover, pH values decreased in the three treatments during the whole incubation, from an initial pH of 8.70 measured in situ to pH 7.89, 7.93, and 7.40, for the treatments OL, OD, and AD, respectively. Eh dropped during the stabilization period (S0), especially in the AD treatment, followed by negative values during S1 and S2, with a small rise after tracer addition.

3.3. Measured rates of N-loss processes

Regarding N-loss processes, the coexistence of denitrification, DNRA, and anammox was confirmed by FISH analyses (Fig. S4). Mean (± standard deviation) and maximum rates are presented in Table 2. Among treatments, significant differences were only found for DNRA ($F_{(2,161)} = 10.0$). Games-Howell post hoc tests indicated DNRA depends on oxygen levels in the water column, distinguishing between AD (2.80 ± 2.56 mmol N m^{-2} h^{-1}) and OL (1.54 ± 1.53 mmol N m^{-2} h^{-1}) or OD (1.35 ± 1.20 mmol N m^{-2} h^{-1}) treatments.

Within each treatment, significant differences were found among processes over time. DNRA and N_2O-denitrification showed significant time-related differences in the OL treatment ($F_{(5,47)}$ of 5.70 and 3.82, respectively). These processes, together with N_2 produced by anammox (hereafter referred to as N_2-anammox) in the interval 3-6 h of incubation, were shown as the dominant ones according to Game-Howell post hoc tests. In the OD treatment, significant differences among processes were found in the interval 3-24 h of incubation. At that time, DNRA and N_2O-denitrification rates were higher than other process rates ($F_{(5,49)}$ of 6.89 and 3.53, respectively). Games-Howell post hoc tests showed that DNRA was the dominant process in the OD treatment between 3 and 6 h of incubation, and then, up to 24 h of incubation, DNRA was co-dominant with N_2O-denitrification. Finally, significant differences were found in the AD treatment between DNRA and the other processes from 3 h of incubation onwards ($F_{(5,50)} = 3.32$). Games-Howell post hoc tests indicated that DNRA was the dominant process up to 48 h.
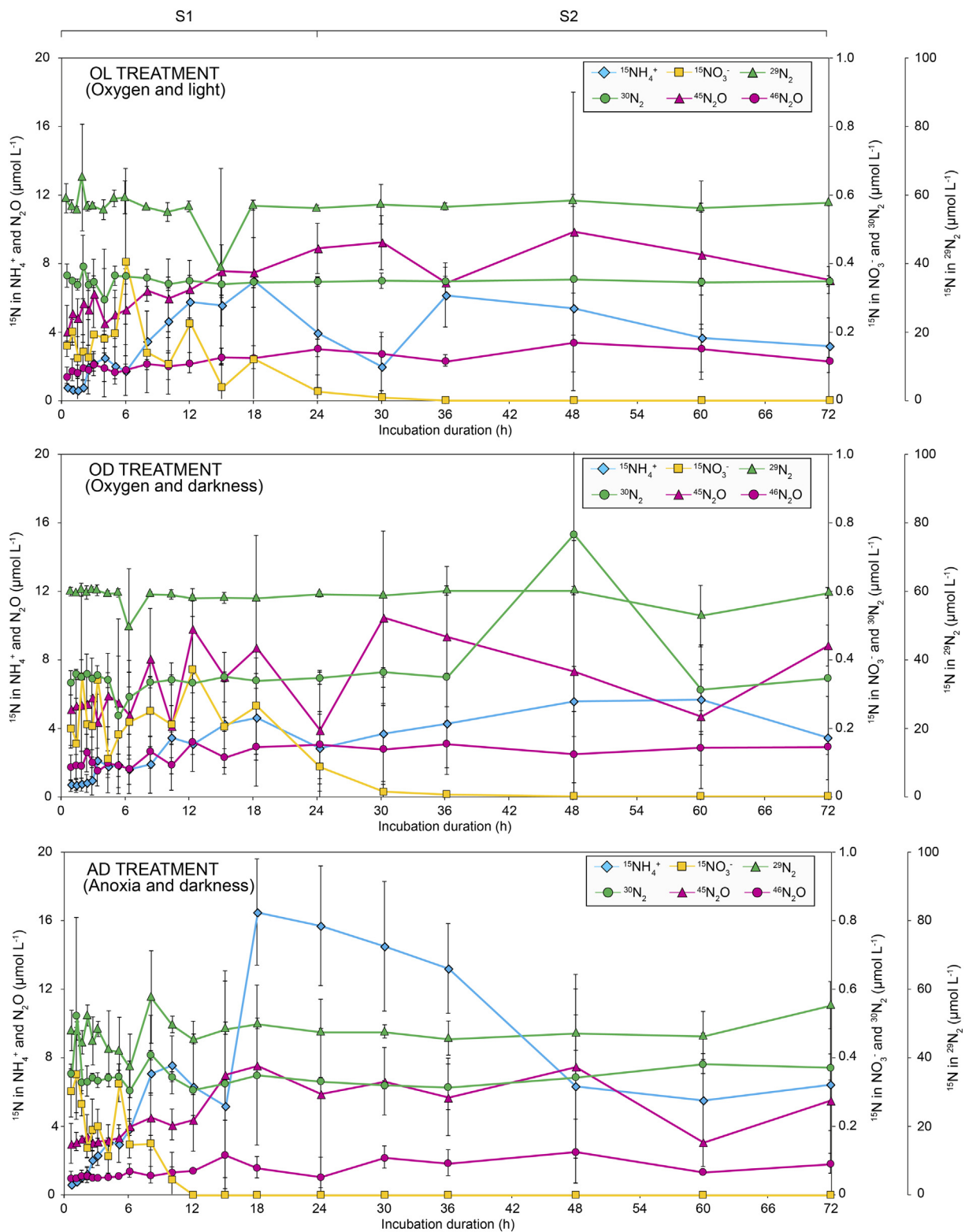
Fig. 1. ^{15}N evolution over time. Changes in $^{15}NH_4^+$, $^{15}NO_3$, $^{29}N_2$, $^{30}N_2$, $^{45}N_2O$ and $^{46}N_2O$ concentration from the time of $^{15}NO_3$ addition onwards (stages S1, 0 - 24 h, and S2, 24 - 72 h). Error bars represent ±1 standard deviation.

4. Discussion

4.1. N-removal over time

The study of N-removal processes in sediment core incubations is often complicated and the processes are hard to measure, due to the high background N_2 concentration in the environment. In recent years, much progress has been made in determining inorganic N processes such as anammox or DNRA using isotopic pairing approaches (Minjeaud et al., 2009; Song et al., 2016; Salk et al., 2017). However, enclosure effects such as the development of anaerobiosis during incubation or the measurement of N_2 have remained problematic, across all

Table 2
Mean (±SD) and maximum rates of N-loss processes after 72 h of mesocosm incubations.

| N-conversion rates (mmol N m^{-2} h^{-1}) | | | | | | | | | | | | | | | | | |
| Mesocosms | Total N removal | | Total NO$_3^-$ reduction | | N$_2$-Denitrification | | N$_2$O-Denitrification | | DNRA-Anammox | | Canonical anammox | | N$_2$-Anammox | | DNRA | |
	Mean	Max	Mean	Max	Mean	Max	Mean	Max	Mean	Max	Mean	Max	Mean	Max	Mean	Max
OL-1 (n = 20)	2.22 (± 2.13)	6.88	3.72 (± 3.26)	10.5	0.13 (± 0.25)	0.85	1.85 (± 1.92)	6.89	0.17 (± 0.34)	1.10	0.07 (± 0.12)	0.42	0.24 (± 0.46)	1.52	1.50 (± 1.57)	5.01
OL-2 (n = 20)	2.16 (± 3.42)	12.3	3.46 (± 4.35)	15.9	0.00 (± 0.02)	0.07	1.39 (± 3.13)	12.3	0.55 (± 0.86)	2.49	0.22 (± 0.40)	1.26	0.77 (± 1.24)	3.38	1.29 (± 1.25)	3.65
OL-3 (n = 20)	2.29 (± 2.62)	9.78	4.09 (± 3.92)	15.1	0.03 (± 0.11)	0.46	2.03 (± 2.69)	9.78	0.15 (± 0.45)	1.66	0.09 (± 0.25)	0.78	0.24 (± 0.70)	2.45	1.80 (± 1.76)	5.59
OL (n = 60)	2.23 (± 2.71)	12.3	3.76 (± 3.79)	15.9	0.05 (± 0.16)	0.85	1.76 (± 2.58)	12.29	0.29 (± 0.61)	2.49	0.12 (± 0.28)	1.26	0.41 (± 0.88)	3.38	1.54 (± 1.53)	5.59
OD-1 (n = 20)	1.54 (± 2.10)	7.65	2.30 (± 2.10)	7.65	0.10 (± 0.28)	1.00	1.43 (± 2.15)	7.65	0.00 (± 0.01)	0.05	0.00 (± 0.01)	0.04	0.01 (± 0.02)	0.09	0.76 (± 0.79)	2.01
OD-2 (n = 20)	2.54 (± 2.56)	11.0	4.33 (± 3.36)	15.4	0.08 (± 0.17)	0.70	1.70 (± 1.55)	5.31	0.41 (± 0.88)	3.62	0.36 (± 0.87)	3.34	0.77 (± 1.72)	6.96	1.79 (± 1.36)	4.41
OD-3 (n = 20)	4.35 (± 4.73)	14.7	5.73 (± 4.92)	16.7	1.03 (± 2.59)	8.33	3.07 (± 2.68)	9.81	0.14 (± 0.57)	2.48	0.11 (± 0.47)	2.05	0.25 (± 1.04)	4.53	1.38 (± 1.16)	3.94
OD (n = 60)	2.87 (± 3.51)	14.7	4.22 (± 3.89)	16.7	0.41 (± 1.57)	8.33	2.10 (± 2.24)	9.81	0.20 (± 0.64)	3.62	0.17 (± 0.60)	3.34	0.37 (± 1.22)	6.96	1.35 (± 1.20)	4.41
AD-1 (n = 20)	4.52 (± 6.00)	21.0	7.41 (± 8.12)	25.3	0.00 (± 0.00)	0.00	4.40 (± 6.00)	21.0	0.08 (± 0.30)	1.33	0.04 (± 0.15)	0.66	0.12 (± 0.45)	1.99	2.89 (± 3.12)	13.9
AD-2 (n = 20)	3.18 (± 5.64)	19.7	6.16 (± 6.14)	22.1	1.79 (± 3.93)	13.0	0.40 (± 1.12)	4.96	0.66 (± 1.51)	5.73	0.33 (± 0.66)	1.84	0.99 (± 2.12)	7.54	2.98 (± 2.21)	8.68
AD-3 (n = 20)	3.16 (± 4.21)	13.5	5.68 (± 5.28)	19.7	0.58 (± 1.95)	8.17	0.75 (± 1.07)	3.97	0.80 (± 1.37)	5.36	1.02 (± 2.26)	7.26	1.82 (± 3.48)	11.0	2.53 (± 2.36)	8.64
AD (n = 60)	3.63 (± 5.30)	21.0	>6.43 (± 6.56)	25.3	0.80 (± 2.61)	13.0	1.87 (± 3.99)	21.0	0.51 (± 1.21)	5.73	0.46 (± 1.38)	7.26	0.96 (± 2.40)	11.0	2.80 (± 2.56)	13.9

incubation methods for decades (Groffman et al., 2006). In our study, to get around these biases, we have combined the gas flow core technique, widely used for the quantification of N$_2$ and N$_2$O production (Wickramasinghe et al., 1978; Nowicki, 1994; Wang et al., 2011; Liao et al., 2013), with a ^{15}N pool dilution approach. The gas flow core technique has several advantages: i) it is non-destructive; ii) no inhibitor is needed; and iii) stable oxygenation conditions can be easily established, which is of significant importance for studies of semi-natural environments. In addition, we addressed the problem of N$_2$ measurement by basing our measurements on N$_2$:Ar ratio measurements (Eyre et al., 2002; Smith et al., 2006; Fulweiler and Nixon, 2012; Zhao et al., 2015).

Three different treatments were applied during the sediment incubations, by modifying oxygen and light conditions in the water column. The darkness treatment mimics the reduction of light derived from enhanced development of planktonic organisms, as commonly observed in shallow eutrophic lakes (Cristofor et al., 1994). In shallow lakes, wind-driven water mixing contributes to avoid anaerobic bottom water conditions (Utsumi et al., 1998). However, shallow eutrophic lakes may exhibit extreme fluctuations in dissolved O$_2$ concentrations, undergoing anoxia as a result of the collapse of phytoplankton blooms (Robarts et al., 2005), together with high sediment oxygen demand (Mallin et al., 2006). These conditions are found in Pétrola Lake, and therefore, the study of the treatments explained above in this study were: OL (oxygen + light), OD (oxygen + darkness), and AD (anoxia + darkness).

Concerning the removal of N, in form of added ^{15}NO$_3^-$, the evolution of N-NO$_3^-$ and N-NO$_2^-$ showed a well-defined NO$_3^-$ reduction pattern in all treatments (Fig. S1). N-NO$_3^-$ decreased during S1, being removed in the first 36 h in the three treatments. This decrease in N-NO$_3^-$ concentrations, together with the intermittent conversion of NO$_3^-$ to NO$_2^-$, suggests the existence of assimilatory and/or dissimilatory NO$_3^-$ reduction processes. In the final stage of the experiment (S2), N-NO$_3^-$ was below LOD. Significant inputs of NO$_3^-$ may also promote phytoplankton blooms of diatoms, what we observed after ^{15}NO$_3^-$ addition in the light treatment (OL). However, N-NO$_3^-$ decreased the fastest in the AD treatment (Fig. S1), suggesting that NO$_3^-$ reduction primarily was driven by heterotrophic bacteria. Thus, the existence of NO$_3^-$ reduction pathways is the most plausible explanation. The decrease in water column pH was probably due to the release of organic acids and CO$_2$, both produced from labile organic carbon during microbial metabolism (Herndon et al., 2015). The existence of microorganisms capable of carrying out these processes was also proven by FISH (Fig. S4). Based on our isotope data, microbially mediated processes (i.e. denitrification, DNRA, and anammox) were responsible for the reduction of the added NO$_3^-$. The average contribution of each process to total N removal and NO$_3^-$ reduction was calculated for each mesocosm and treatment (Fig. 2). Furthermore, the evolution of the participation of each pathway to NO$_3^-$ reduction is shown in Fig. 3.

As stated above, a sharp decrease in N-NO$_3^-$ concentration was observed in all the treatments after the addition of the tracer. Simultaneously, there was no accumulation of N-NO$_2^-$ in the water column, which suggests the rapid consumption of NO$_2^-$ by both, denitrification and anammox. On average, anammox cooontributed less to total N removal compared to denitrification (Fig. 2). However, its contribution to NO$_3^-$ reduction was most relevant in the first hours of incubation: up to 6 h in the OL treatment (on average 18.0%), up to 2.5 h in the OD treatment (on average 20.1%), and up to 4 h in the AD treatment (on average 18.1%) (Fig. 3). However, anammox lost prominence over time in the first two treatments. In parallel, a remarkable accumulation of N-NH$_4^+$ in the water column was observed in all treatments from time 0 onwards. Although processes such as OM remineralization and sedimentary release may increase NH$_4^+$ in the water column (Kalvelage et al., 2013), DNRA seems to have played the crucial role in the NH$_4^+$ accumulation. During the stabilization period (S0 stage), the absence of NO$_3^-$ may have hindered the activity of
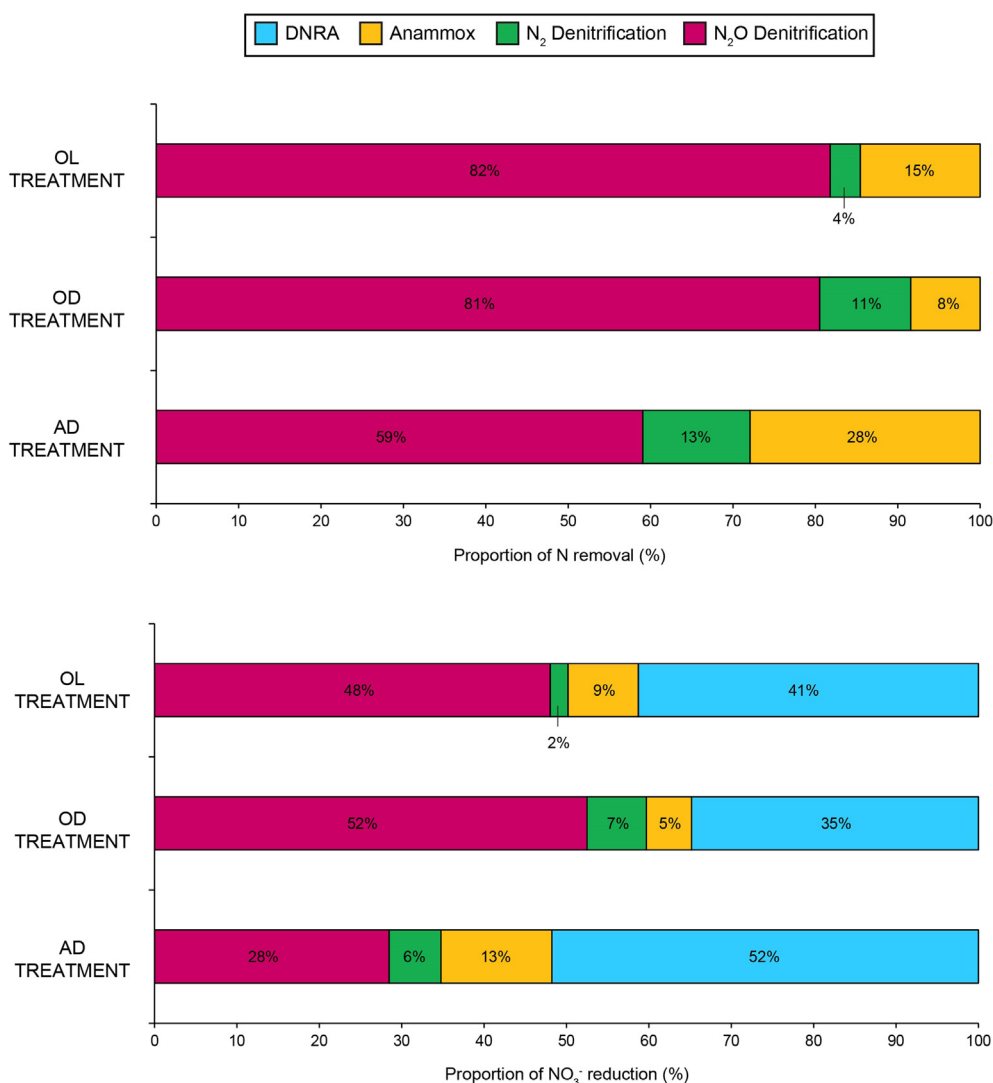
Fig. 2. Contribution of each pathway to total N removal and to NO_3^- reduction. Proportion of N_2-denitrification, N_2O-denitrification, and anammox to total N removal (left). Contribution of DNRA, N_2-denitrification, N_2O-denitrification, and anammox to NO_3^- reduction (right). Rates were measured under three different incubation conditions (treatments OL, OD, and AD).

DNRA bacteria, and the increase of NH_4^+ in the water column must therefore be a consequence of the rapid release from decaying cyanobacteria, as demonstrated by others (Gao et al., 2013). The small oscillations observed through S1 (up to 24 h) were the result of fluctuations in $N-NH_4^+$ production (DNRA and water-column OM remineralization) and consumption (anammox, NH_4^+ assimilation, and nitrification). The contribution of anammox to total N removal has already been highlighted during the first hours after tracer addition. Regarding DNRA, its contribution to NO_3^- reduction reached maximum values during the same period: 60.2% in the OL treatment (at 4 h), 65.9% in the OD treatment (at 5 h), and 80.0% in the AD treatment (at 4 h). While DNRA was the major NO_3^- reduction pathway during the whole S1 period in the AD treatment (on average 50.0%), this was not the case for the OL and OD treatments (on average 42.1% and 37.8%, respectively). DNRA remained the major NO_3^- reduction pathway in the AD treatment during the S2 period (on average 56.7%), providing the highest $N-NH_4^+$ concentrations at the end of the incubation (198 ± 12.2 μmol/L; Table 1). Although DNRA was not the main process in the OL and OD treatments, $N-NH_4^+$ accumulation in the water column was observed through S1 and S2 stages, which can be also attributed to sedimentary OM remineralization after algal bloom collapse (García-Robledo and Corzo, 2011). This can be supported by DOC and DON measurements. A sharp increase of DOC was observed in all the treatments

during the S1 stage (Fig. S3), which likely derived from the phytoplankton bloom collapse. Afterwards, DOC concentrations decreased as a result of heterotrophic bacterial metabolism. DON values also supported this, as the decreasing DON:DNb ratios underline the role of OM remineralization throughout the incubation (Table 1).

Concentrations of N_2 remained almost constant throughout the incubations ($\approx$ 6 mmol/L; Fig. S1). N_2 oversaturation may result from inorganic N reduction processes and N_2 accumulation in the water column, when atmospheric equilibrium has not yet been reached (Weiss and Craig, 1973; Wenk et al., 2013, 2014). Small changes in both $^{29}N_2$ and $^{30}N_2$ were observed after the addition of $^{15}NO_3^-$. During the hours after the tracer addition, the production of $^{30}N_2$ can be attributed either to denitrification or to coupled DNRA-anammox, by combining the DNRA substrate ($^{15}NO_2^-$) with the DNRA product ($^{15}NH_4^+$) (Holtappels et al., 2011). In the OD treatment, a sharp increase in $^{29}N_2$ was observed after 48 h, which is attributed to denitrification or to canonical anammox (Song et al., 2016). This is also supported by Fig. 3, as at this time both processes accounted for 10.1% of total NO_3^- reduction. In contrast, the evolution of N_2O showed an accumulation of total N_2O over time, especially in the OD and AD treatments (Fig. S1). N_2O-denitrification was the main N removal pathway (Fig. 2). However, increases in both $^{45}N_2O$ and $^{46}N_2O$ over time did not follow the same trend as total N_2O, which is discussed below.
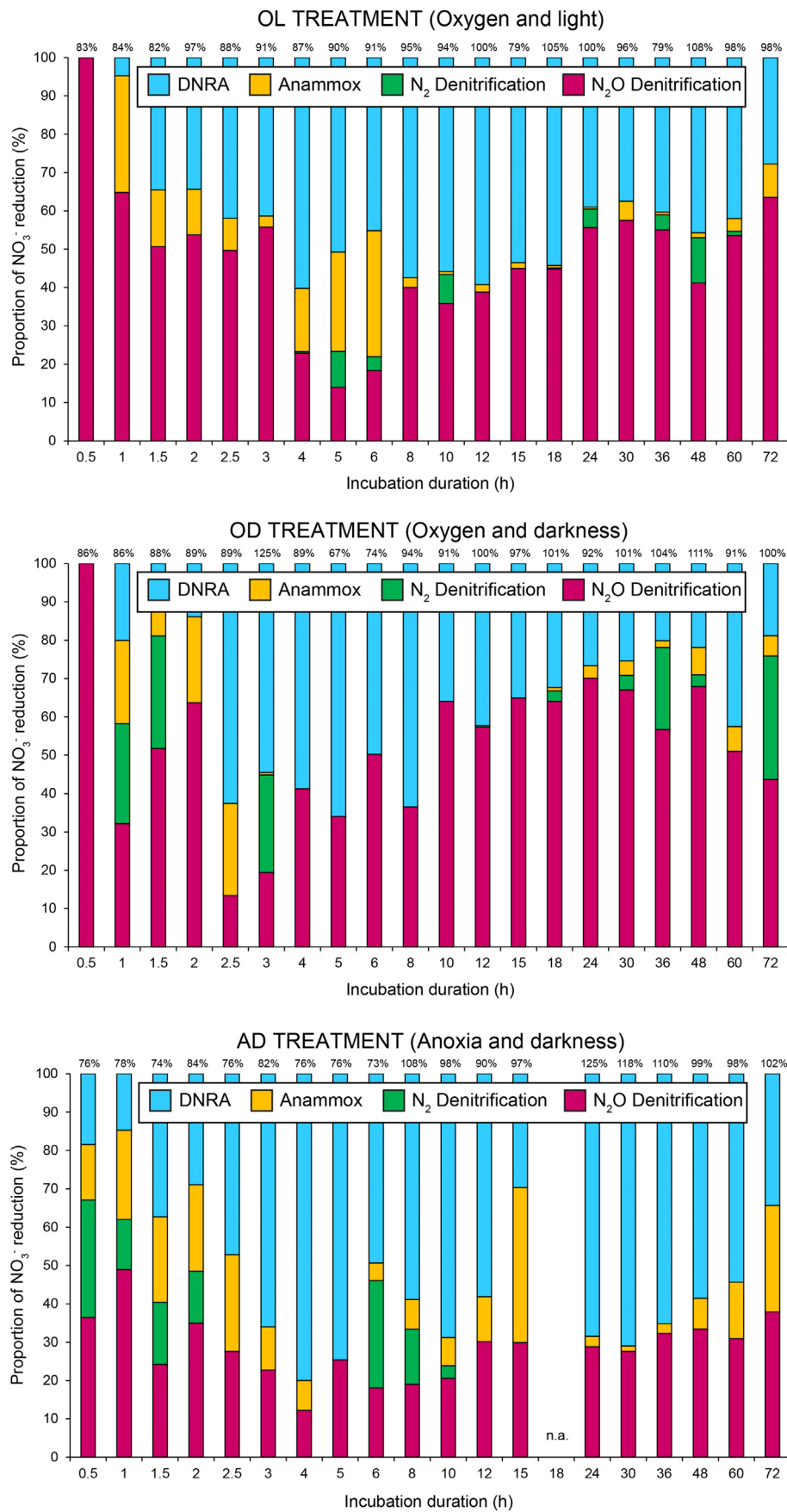
Fig. 3. Evolution of the contribution to NO$_3^-$ reduction over time. Proportion of N$_2$-denitrification, N$_2$O-denitrification, DNRA, and anammox under three incubation conditions (treatments OL, OD, and AD). Proportions of each process were measured at twenty different incubation times, in triplicate per treatment and time. Recovery percentages of initial ^{15}N added at each time is shown above the bars. Detailed mass balances are reported in Fig. S2. n.a.: not available.

4.2. N$_2$O production

A general increase in N$_2$O over time was observed in all the treatments (Fig. S1). ANOVA results shown in Section 3.3 provided evidence of a (co-) dominant role of N$_2$O-denitrification in the OL and OD treatments, accounting for 82% and 81% of N removal, respectively (Fig. 2). The contribution of N$_2$O-denitrification to total N loss was significantly higher than reported for aquatic sediments in other studies (< 8.6%; Risgaard-Petersen et al., 2003; McCrackin and Elser, 2010). The treatments OL and OD showed mean N$_2$O-denitrification rates of 1.76 ($\pm$ 2.58) and 2.10 ($\pm$ 2.24) mmol N m^{-2} h^{-1}, respectively. Such high values have been reported previously only in tropical wetland soils (up to 1.56 mmol N m^{-2} h^{-1}; Liengaard et al., 2014) and estuarine sediments affected by agricultural activities (up to 4.85 mmol N m^{-2} h^{-1}; Salahudeen et al., 2018) (Table 3). These results support the evidence from previous observations (Huttunen et al., 2003), which showed that lakes subjected to elevated N inputs are an important source of N$_2$O emissions.

The AD treatment showed a similar average value of N$_2$O-denitrification (1.87 $\pm$ 3.99 mmol N m^{-2} h^{-1}) as the treatments OL and OD, being similar to rates reported for pristine mangrove sediments (up to 0.67 mmol N m^{-2} h^{-1}; Fernandes et al., 2010), but higher rates of N$_2$-denitrification than OL and OD. Therefore, N$_2$O-denitrification showed a smaller yet still dominant contribution to total N removal in the AD treatment. A possible explanation for this pattern is that N$_2$O reductase activity is sensitive towards oxygen (Bonin and Gilewicz, 1991), being partially inhibited in the treatments OL and OD in the presence of dissolved O$_2$ (~ 6.4 mg/L in the water column), thereby inhibiting N$_2$-denitrification under aerated conditions. Overall, N$_2$O-denitrification showed a significant contribution to NO$_3^-$ reduction during the whole sediment incubations, together with DNRA (Fig. 3). In terms of NO$_3^-$ reduction, when N$_2$O-denitrification was of greater importance, DNRA and anammox showed a smaller contribution to NO$_3^-$ reduction, and vice versa. N$_2$O-denitrification showed the lowest contribution to NO$_3^-$ reduction when DNRA and anammox were of greater importance. The contribution of N$_2$O-denitrification dropped to 14.0% in the OL treatment (at 5 h), 13.4% in the OD treatment (at 2.5 h) and 12.2% in the AD treatment (at 4 h). These results support previous studies that have shown that denitrification and DNRA compete for oxidized N compounds (van den Berg et al., 2017a, 2017b).

Studies on the role of N$_2$O-denitrification in saline aquatic environments are mainly restricted to marine ecosystems. The high measured rates in this hypersaline lake may be explained by the combination of: i) high biological activity after ^{15}NO$_3^-$ addition in the absence of nutrient limitation; and ii) low N$_2$O reductase activity in the OL and OD treatments. If denitrification was the sole source of N$_2$ and N$_2$O, the different patterns observed for ^{29}N$_2$ and ^{45}N$_2$O (Fig. 1) cannot be explained, as the proportions of ^{29}N$_2$ and ^{30}N$_2$ at steady state conditions would match the proportions of ^{45}N$_2$O and ^{46}N$_2$O (Trimmer et al., 2006). Differences in ^{29}N$_2$ and ^{45}N$_2$O can be attributed to anammox due to an imbalance of the proportion of ^{15}N by producing ^{29}N$_2$. However, nitrification also produces N$_2$O during its first step. This step involves the oxidation of ammonia (NH$_3$) to NO$_2^-$ by ammonia-oxidizing archaea (AOA) and ammonia-oxidizing bacteria (AOB). To reveal the contribution to N$_2$O production by ammonia oxidation through AOA and AOB, we calculated gross nitrification rates based on isotope dilution principles. Unfortunately, the obtained rates were below LOD, meaning that nitrification plays a minor role in this system. In order to shed light on it, another type of mesocosm experiments would be needed to measure the contribution of ammonia oxidizers to N$_2$O production, which was not the focus of this study.

During N$_2$ production, the evolution of ^{29}N$_2$ and ^{30}N$_2$ over time was highly similar (Fig. 1), suggesting a common production mechanism. According to IPT calculations, N$_2$-denitrification showed the highest rates at the beginning of the incubation (AD, $\leq$ 13 mmol N m^{-2} h^{-1}). The mean N$_2$ production rate attributed to denitrification in the OL treatment was 0.05 mmol N m^{-2} h^{-1}, in accordance with intact estuarine sediments (0.036–0.155 mmol N m^{-2} h^{-1}; Trimmer et al., 2003), and contributed on average 4% to total N removal (Fig. 2). N$_2$-denitrification played a greater role in NO$_3^-$ reduction under darkness, removing 11% and 13% of the total N in the OD and AD treatments, respectively. These results agree with earlier observations (Risgaard-Petersen et al., 1994), which showed reduced denitrification rates associated with light exposure and photosynthesis by benthic microphytes. In the OD treatment, the mean production rate was 0.41 ($\pm$ 1.57) mmol N m^{-2} h^{-1} by N$_2$-denitrification (Table 2). These values are similar to those reported for marine environments, like Heron Island (0.48 mmol N m^{-2} h^{-1}; Eyre and Ferguson, 2009) and Randers Fjord (0.34 mmol N m^{-2} h^{-1}; Risgaard-Petersen et al., 2004) (Table 3). Highest N$_2$-denitrification rates were found in the AD treatment, with an average value of 0.80 ($\pm$ 2.61) mmol N m^{-2} h^{-1}. These results are close to those reported by Erler et al. (2008) (0.652–0.966 mmol N m^{-2} h^{-1}), where denitrifiers coexisted with anammox bacteria in a constructed wetland, which received secondary treated sewage effluents. The

Table 3
Published rates of sedimentary denitrification, DNRA and anammox measured in intact sediment cores (mmol N m^{-2} h^{-1}). n.a.: not available.

Source	DNRA	Anammox	N$_2$-Denitrification	N$_2$O-Denitrification	Reference
Pétrola Lake (Spain)	0 - 2.800	0 - 0.960	0 - 0.800	0 - 2.100	This study
Colne estuary (United Kingdom)	0.005 - 0.400	0.157	n.a.	n.a.	Dong et al. (2009)
Cisadane estuary (Indonesia)	1.140	n.a.	n.a.	n.a.	Dong et al. (2011)
Thau lagoon (France)	6.708	n.a.	n.a.	n.a.	Gilbert et al. (1997)
East China Sea shelf (China)	0.791 - 3.583	n.a.	n.a.	n.a.	Song et al. (2013)
Fringing marsh-aquifer ecotone (USA)	0.875 - 6.125	n.a.	1.800 - 17.60	n.a.	Tobias et al. (2001)
Plum Island Sound estuary (USA)	0.004 - 0.310	n.a.	0 - 0.332	n.a.	Koop-Jakobsen and Giblin (2010)
German Bight (Germany)	0.010	n.a.	0.124	n.a.	Marchant et al. (2016)
Heron Island (Australia)	n.a.	n.a.	0.034 - 0.480	n.a.	Eyre and Ferguson (2009)
Lake Tanganyika (Burundi, DRC, Tanzania, Zambia)	n.a.	0.100	n.a.	n.a.	Schubert et al. (2006)
Randers Fjord (Denmark)	n.a.	0.014 - 0.021	0.219 - 0.335	n.a.	Risgaard-Petersen et al. (2004)
Thames estuary (United Kingdom)	n.a.	0 - 0.010	0.036 - 0.155	n.a.	Trimmer et al. (2003)
Gravesend, Thames estuary (United Kingdom)	n.a.	0.049	0.193	n.a.	Trimmer et al. (2006)
Constructed wetland in New South Wales (Australia)	n.a.	0.066 - 0.199	0.652 - 0.966	n.a.	Erler et al. (2008)
Taihu Lake (China)	n.a.	0.049 - 0.413	0.132 - 0.656	n.a.	Han and Li (2016)
Lake Superior (Canada, USA)	n.a.	0.021 - 0.040	0.019 - 0.128	n.a.	Crowe et al. (2017)
Danshuei estuary (Taiwan)	n.a.	0.013	0.126	0.050	Hsu and Kao (2013)
Pearl River estuary (China)	n.a.	0 - 0.003	0.032 - 0.708	0 - 0.022	Tan et al. (2019)
Lake Bonney (Antarctica)	n.a.	n.a.	n.a.	0.191	Prisu et al. (1996)
Tuvem and Divar, Goa (India)	n.a.	n.a.	n.a.	0.140 - 0.670	Fernandes et al. (2010)
Pantanal wetland (Brazil)	n.a.	n.a.	n.a.	0 - 1.560	Liengaard et al. (2014)
Ashtamudi estuary (India)	n.a.	n.a.	n.a.	0.490 - 4.850	Salahudeen et al. (2018)

largest contribution of N_2-denitrification was detected at the initial phase of incubation, coupled to higher DOC concentrations, but also during later phases of incubation in the OD treatment (~ 30%) (Fig. 3). These results suggest the dominance of heterotrophic denitrifiers, linked to the breakdown of biomass derived from phytoplankton collapse (Xue et al., 2017). Sharp increases in N_2 concentration were found at different times in the OL treatment (7.51 mmol/L, time 6 h), the OD treatment (13.3 mmol/L, time 48 h), and in the AD treatment (6.87 mmol/L, time 8 h). These high rates coincided with incubation times with high N_2-denitrification and anammox rates (Fig. 3). Their combined contribution to NO_3^- reduction was on average 35.9% in the OL treatment (times 5 h and 6 h), 16.6% in the OD treatment (times 36 h and 48 h) and 27.4% in the AD treatment (times 6 h and 8 h).

4.3. Close coupling between DNRA and anammox

Total N removal and NO_3^- reduction reached highest values under anoxia and darkness conditions (mean of 3.63 ± 5.30 mmol N m^{-2} h^{-1} and 6.43 ± 6.56 mmol N m^{-2} h^{-1}, respectively; Table 2). As discussed above, under those conditions DNRA was the dominant process. These results are consistent with hydrochemical data, which showed a significant accumulation of N-NH_4^+ in the water column in the AD treatment. Previous research showed favorable conditions for DNRA activity in sediments from Pétrola Lake, such as high organic C:N ratios and the presence of microorganisms capable of performing DNRA (Valiente et al., 2017; Valiente et al., 2018). Average DNRA rates in the OL and OD treatments (~ 1.4 mmol N m^{-2} h^{-1}) are similar to those reported for anoxic estuarine sediments, where DNRA is the dominant process (1.140 mmol N m^{-2} h^{-1}; Dong et al., 2011). In the AD treatment, mean DNRA rates (2.80 ± 2.56 mmol N m^{-2} h^{-1}) were similar to those observed in nutrient enriched environments, like fringing wetlands (up to 6.13 mmol N m^{-2} h^{-1}; Tobias et al., 2001) and eutrophic shelf seas (up to 3.58 mmol N m^{-2} h^{-1}; Song et al., 2013) (Table 3). ANOVA tests (Section 3.3) showed that NO_3^- reduction by DNRA was significantly higher in the AD treatment (52%) than in the OL (41%) and the OD treatments (35%) (Fig. 2). The contribution of DNRA was in the same range as reported for estuarine and salt marsh sediments (Dong et al., 2009; Koop-Jakobsen and Giblin, 2010), fostering the retention of reactive N in the system. As discussed above, DNRA contributed more to NO_3^- reduction after the initial incubation phase, approximately from time 2.5 h onwards (Fig. 3). Recent studies also demonstrated that DNRA is stimulated in the presence of H_2S at the expense of denitrification (Roland et al., 2018). Our results support those findings: the AD treatment provided the most favorable conditions for bacterial sulfate-reduction (Table 1), and H_2S production in Pétrola sediments (Valiente et al., 2017) can reach values up to 0.024 $nmol/cm^3$·s.

Existing NH_4^+ can be oxidized to NO_2^-, both under aerobic and anaerobic conditions (Schmidt et al., 2002), contributing to a temporary increase of N-NO_2^- and promoting NO_2^- and NH_4^+ consumption by anammox bacteria. Moreover, N-NH_4^+ release does fuel N loss from the system via coupled DNRA-anammox. For instance, anammox reached up to 40.4% of total reduction in the AD treatment at time 15 h. Simultaneously, we found significant concentrations of both N-NO_2^- (29.6 $\mu mol/L$) and N-NH_4^+ (138.4 $\mu mol/L$). Therefore, DNRA and anammox bacteria, acting together, may have an energetic advantage over denitrifiers in the competition for substrates under low oxygen conditions (Jensen et al., 2011). Such a close reliance of anammox organisms on DNRA bacteria has been reported in marine ecosystems with high N loss via anammox, mainly linked to high availability of OM (Kalvelage et al., 2013). In Pétrola Lake sediment incubations, anammox bacteria seem to be fueled by a DNRA process. This interpretation is based on the similar trend of the contribution of both processes to total NO_3^- reduction (AD>OL > OD; Fig. 2). Coupled DNRA-anammox showed a higher contribution in all treatments than canonical anammox (Table 2), corroborating the key role of DNRA in fueling N loss pathways.

The isotope data clearly confirm the presence of anammox (Table 2). The mean rates of N loss via anammox in the OL and OD treatments (~0.4 mmol N m^{-2} h^{-1}) were in the range of previous studies in eutrophic sediments (up to 0.41 mmol N m^{-2} h^{-1}; Han and Li, 2016), but significantly lower than those found in the AD treatment (0.96 mmol N m^{-2} h^{-1}). These results agree with recent studies, showing the importance of anammox activity in the presence of H_2S in freshwater lakes (Roland et al., 2018), conditions which are given for the highly saline lake studied here. On average, the contribution of anammox to total N loss ranged from 8% (OD) to 28% (AD) (Fig. 2). This range corresponds with studies performed in continental shelf sediments (Song et al., 2013) (28%), intertidal sediments (Hsu and Kao, 2013) (12%), and is close to the global mean value, including inland waters (Trimmer and Engström, 2011) (23%).

These findings provide a better understanding of the contribution of DNRA and anammox to inorganic N removal in inland waters in general, and in particular for saline lakes. In eutrophic systems, where important environmental factors (i.e. nutrients, light, oxygen) are limiting, the development of phytoplankton blooms is favored. When the algal bloom collapses, the resulting decomposition of OM fosters microbial activity, and as our findings showed, the production of N_2O as a by-product of the reduction of existing NO_3^-. Given the environmental implications of N_2O (Ravishankara et al., 2009), these emissions to the atmosphere need to be avoided. When light is a limiting factor (e.g. surface blooms, browning), our results showed that N_2O production is still a major contributor to NO_3^- removal, but DNRA became less significant (which is not necessarily desirable). Finally, when both oxygen and light were constraining factors, competition between denitrification and DNRA favored the latter, in turn boosting the rate of anammox. If both DNRA and anammox are coupled (i.e. NH_4^+ does not accumulate in the system), the proportion of N_2O-denitrification decreased and the production of N_2 increased as a result of N_2-denitrification and anammox (Fig. 2). In fact, the higher the contribution of anammox to total N removal was, the lower the relevance of N_2O-denitrification became. Anoxia and darkness, that are in principle "undesirable" conditions, not only stimulated NO_3^- reduction by coupled DNRA-anammox, but also restricted the contribution of other processes like denitrification to N_2O production. Therefore, these conditions are likely to stimulate a self-regulation mechanism by accelerating the elimination of nutrients and reducing the release of N_2O to the atmosphere.

5. Conclusions

The purpose of the current study was to determine the different ways, in which NO_3^- is removed in lacustrine organic-rich sediments, and how oxygen and light in the water column affect the balance between those NO_3^- removal pathways. Our findings provide the first evidence for the coexistence of denitrification, DNRA, and anammox in a highly saline lake. In addition, our experiments applying the revised ^{15}N-IPT showed the importance of coupled DNRA-anammox, which has not yet been investigated in lacustrine sediments. We showed here that N_2O-denitrification played a predominant role in N removal, with unexpected high N_2O emission rates compared to previous studies. In addition, DNRA was the key process, when oxygen and light were absent from the water column. Under these conditions, anammox also had a greater influence on total N removal, with markedly high rates (up to 0.96 mmol N m^{-2} h^{-1}). Therefore, anoxia and darkness promoted DNRA against denitrification, which is critical to fuel anammox. As a result, these conditions limited N_2O emissions to the atmosphere. Further research is required to fully understand the role of coupled DNRA-anammox in N cycling in lake ecosystems, as well as the influence that coupled DNRA-nitrification can exert on N_2O production.

CRediT authorship contribution statement

NV, FJ, TH and JJGA designed the study. NV performed the experiment. NV, FJ, WW and PB analyzed the samples. NV, JP, WW, PB and

JJGA conducted the data analysis. NV led the writing of the manuscript, with substantial contributions from all coauthors.

Declaration of competing interest

The authors declare that they have no known competing financial interests or personal relationships that could have appeared to influence the work reported in this paper.

Appendix A. Supplementary data

Supplementary data to this article can be found online at https://doi.org/10.1016/j.scitotenv.2021.150726.

References

Abed, R.M.M., de Beer, D., Stief, P., 2015. Functional-structural analysis of nitrogen-cycle bacteria in a hypersaline mat from the Omani Desert. Geomicrobiol. J. 32 (2), 119–129. https://doi.org/10.1080/01490451.2014.932033.

Bonin, P., Gilewicz, M., 1991. A direct demonstration of "co-respiration" of oxygen and nitrogen oxides by Pseudomonas nautica: some spectral and kinetic properties of the respiratory components. FEMS Microbiol. Lett. 80 (2–3), 183–188. https://doi.org/10.1111/j.1574-6968.1991.tb04658.x.

Bonin, P., Omnes, P., Chalamet, A., 1999. The influence of nitrate and carbon inputs on the end products of bacterial nitrate dissimilation in marine sediment. Toxicol. Environ. Chem. 73 (1–2), 67–79. https://doi.org/10.1080/02772249909358848.

Brooks, P.D., Stark, J.M., McInteer, B.B., Preston, T., 1989. Diffusion method to prepare soil extracts for automated nitrogen–15 analysis. Soil Sci. Soc. Am. J. 53, 1707–1711. https://doi.org/10.2136/sssaj1989.03615995005300060016x.

Cristofor, S., Vadineanu, A., Ignat, G., Ciubuc, C., 1994. Factors affecting light penetration in shallow lakes. Hydrobiologia 275 (1), 493–498. https://doi.org/10.1007/BF00026737.

Crowe, S.A., Treusch, A.H., Forth, M., Li, J., Magen, C., Canfield, D.E., Thamdrup, B., Katsev, S., 2017. Novel anammox bacteria and nitrogen loss from Lake Superior. Sci. Rep. 7 (1), 13757. https://doi.org/10.1038/s41598-017-12270-1.

Dalsgaard, T., Nielsen, L., Brotas, V., Viaroli, P., Underwood, G., Nedwell, D., Sundbäck, K., Rysgaard, S., Miles, A., Bartoli, M., et al., 2000. Ministry of Environment and Energy National Environmental Research Institute, Denmark, p. 62.

Deng, F., Hou, L., Liu, M., Zheng, Y., Yin, G., Li, X., Lin, X., Chen, F., Gao, J., Jiang, X., 2015. Dissimilatory nitrate reduction processes and associated contribution to nitrogen removal in sediments of the Yangtze Estuary. J. Geophys. Res. Biogeosci. 120, 1521–1531. https://doi.org/10.1002/2015JG003007.

Doi, H., Kikuchi, E., Mizota, C., Satoh, N., Shikano, S., Yurlova, N., Yadrenkina, E., Zuykova, E., 2004. Carbon, nitrogen, and sulfur isotope changes and hydro-geological processes in a saline lake chain. Hydrobiologia 529 (1), 225–235. https://doi.org/10.1007/s10750-004-6418-2.

Dong, L.F., Smith, C.J., Papaspyrou, S., Stott, A., Osborn, A.M., Nedwell, D.B., 2009. Changes in benthic denitrification, nitrate ammonification, and anammox process rates and nitrate and nitrite reductase gene abundances along an estuarine nutrient gradient (the colne estuary, United Kingdom). Appl. Environ. Microbiol. 75 (10), 3171. https://doi.org/10.1128/AEM.02511-08.

Dong, L.F., Sobey, M.N., Smith, C.J., Rusmana, I., Phillips, W., Stott, A., Osborn, A.M., Nedwell, D.B., 2011. Dissimilatory reduction of nitrate to ammonium, not denitrification or anammox, dominates benthic nitrate reduction in tropical estuaries. Limnol. Oceanogr. 56 (1), 279–291. https://doi.org/10.4319/lo.2011.56.1.0279.

Erler, D.V., Eyre, B.D., Davison, L., 2008. The contribution of anammox and denitrification to sediment N2 production in a surface flow constructed wetland. Environ. Sci. Technol. 42 (24), 9144–9150. https://doi.org/10.1021/es801175t.

Eyre, B.D., Ferguson, A.J.P., 2009. Denitrification efficiency for defining critical loads of carbon in shallow coastal ecosystems. In: Andersen, J.H., Conley, D.J. (Eds.), Eutrophication in Coastal Ecosystems: Towards better understanding and management strategies Selected Papers from the Second International Symposium on Research and Management of Eutrophication in Coastal Ecosystems, 20–23 June 2006, Nyborg, Denmark. Springer, Netherlands, Dordrecht, pp. 137–146.

Eyre, B.D., Rysgaard, S., Dalsgaard, T., Christensen, P.B., 2002. Comparison of isotope pairing and N2: ar methods for measuring sediment denitrification—assumption, modifications, and implications. Estuaries 25 (6), 1077–1087. https://doi.org/10.1007/BF02692205.

Fernandes, S.O., Bharathi, P.A.L., Bonin, P.C., Michotey, V.D., 2010. Denitrification: an important pathway for nitrous oxide production in tropical mangrove sediments (Goa, India). J. Environ. Qual. 39 (4), 1507–1516. https://doi.org/10.2134/jeq2009.0477.

Fernandes, S.O., Michotey, V.D., Guasco, S., Bonin, P.C., Bharathi, P.L., 2012. Denitrification prevails over anammox in tropical mangrove sediments (Goa, India). Mar. Environ. Res. 74, 9–19. https://doi.org/10.1016/j.marenvres.2011.11.008.

Fernandes, S.O., Javanaud, C., Michotey, V.D., Guasco, S., Anschutz, P., Bonin, P., 2016. Coupling of bacterial nitrification with denitrification and anammox supports N removal in intertidal sediments (Arcachon Bay, France). Estuar. Coast. Shelf Sci. 179, 39–50. https://doi.org/10.1016/j.ecss.2015.10.009.

Francis, C.A., Beman, J.M., Kuypers, M.M.M., 2007. New processes and players in the nitrogen cycle: the microbial ecology of anaerobic and archaeal ammonia oxidation. ISME J. 1 (1), 19–27. https://doi.org/10.1038/ismej.2007.8.

Fulweiler, R.W., Nixon, S.W., 2012. Net sediment N2 fluxes in a southern New England estuary: variations in space and time. Biogeochemistry 111 (1–3), 111–124. https://doi.org/10.1007/s10533-011-9660-5.

Gao, L., Zhang, L., Hou, J., Wei, Q., Fu, F., Shao, H., 2013. Decomposition of macroalgal blooms influences phosphorus release from the sediments and implications for coastal restoration in Swan Lake, Shandong, China. Ecol. Eng. 60, 19–28. https://doi.org/10.1016/j.ecoleng.2013.07.055.

García-Robledo, E., Corzo, A., 2011. Effects of macroalgal blooms on carbon and nitrogen biogeochemical cycling in photoautotrophic sediments: an experimental mesocosm. Mar. Pollut. Bull. 62 (7), 1550–1556. https://doi.org/10.1016/j.marpolbul.2011.03.044.

García-Robledo, E., Corzo, A., Papaspyrou, S., 2014. A fast and direct spectrophotometric method for the sequential determination of nitrate and nitrite at low concentrations in small volumes. Mar. Chem. 162, 30–36. https://doi.org/10.1016/j.marchem.2014.03.002.

Gilbert, F., Souchu, P., Bianchi, M., Bonin, P., 1997. Influence of shellfish farming activities on nitrification, nitrate reduction to ammonium and denitrification at the water-sediment interface of the Thau lagoon, France. Mar. Ecol. Prog. Ser. 151, 143–153. https://doi.org/10.3354/meps151143.

Gómez-Alday, J.J., Carrey, R., Valiente, N., Otero, N., Soler, A., Ayora, C., Sanz, D., Muñoz-Martín, A., Castaño, S., Recio, C., Carnicero, A., Cortijo, A., 2014. Denitrification in a hypersaline lake–aquifer system (Pétrola Basin, Central Spain): the role of recent organic matter and cretaceous organic rich sediments. Sci. Total Environ. 497–498, 594–606. https://doi.org/10.1016/j.scitotenv.2014.07.129.

Groffman, P.M., Altabet, M.A., Böhlke, J.K., Butterbach-Bahl, K., David, M.B., Firestone, M.K., Giblin, A.E., Kana, T.M., Nielsen, L.P., Voytek, M.A., 2006. Methods for measuring denitrification: diverse approaches to a difficult problem. Ecol. Appl. 16 (6), 2091–2122. https://doi.org/10.1890/1051-0761(2006)016[2091:MFMDDA]2.0.CO;2.

Hallin, S., Philippot, L., Löffler, F.E., Sanford, R.A., Jones, C.M., 2018. Genomics and ecology of novel N2O-reducing microorganisms. Trends Microbiol. 26 (1), 43–55. https://doi.org/10.1016/j.tim.2017.07.003.

Hamme, R.C., Emerson, S.R., 2004. The solubility of neon, nitrogen and argon in distilled water and seawater. Deep-Sea Res. I Oceanogr. Res. Pap. 51 (11), 1517–1528. https://doi.org/10.1016/j.dsr.2004.06.009.

Han, H., Li, Z., 2016. Effects of macrophyte-associated nitrogen cycling bacteria on ANAMMOX and denitrification in river sediments in the Taihu Lake region of China. Ecol. Eng. 93, 82–90. https://doi.org/10.1016/j.ecoleng.2016.05.015.

Harrison, J.A., Maranger, R.J., Alexander, R.B., Giblin, A.E., Jacinthe, P.-A., Mayorga, E., Seitzinger, S.P., Sobota, D.J., Wollheim, W.M., 2009. The regional and global significance of nitrogen removal in lakes and reservoirs. Biogeochemistry 93 (1), 143–157. https://doi.org/10.1007/s10533-008-9272-x.

Herndon, E.M., Mann, B.F., RoyChowdhury, T., Yang, Z., Wullschleger, S.D., Graham, D., Liang, L., Gu, B., 2015. Pathways of anaerobic organic matter decomposition in tundra soils from Barrow, Alaska. J. Geophys. Res. Biogeosci. 120, 2345–2359. https://doi.org/10.1002/2015JG003147.

Holtappels, M., Lavik, G., Jensen, M.M., Kuypers, M.M.M., 2011. Chapter ten - 15N-labeling experiments to dissect the contributions of heterotrophic denitrification and anammox to nitrogen removal in the OMZ waters of the ocean. In: Klotz, M.G. (Ed.), Methods in Enzymology. 486. Academic Press, pp. 223–251.

Hood-Nowotny, R., Umana, N.H.-N., Inselbacher, E., Oswald- Lachouani, P., Wanek, W., 2010. Alternative methods for measuring inorganic, organic, and total dissolved nitrogen in soil. Soil Sci. Soc. Am. J. 74 (3), 1018–1027. https://doi.org/10.2136/sssaj2009.0389.

Hsu, T.-C., Kao, S.-J., 2013. Technical note: simultaneous measurement of sedimentary N2 and N2O production and a modified 15N isotope pairing technique. Biogeosciences 10 (12), 7847–7862. https://doi.org/10.5194/bg-10-7847-2013.

Huttunen, J.T., Juutinen, S., Alm, J., Larmola, T., Hammar, T., Silvola, J., Martikainen, P.J., 2003. Nitrous oxide flux to the atmosphere from the littoral zone of a boreal lake. J. Geophys. Res. Atmos. 108 (D14).

Jensen, M.M., Lam, P., Revsbech, N.P., Nagel, B., Gaye, B., Jetten, M.S., Kuypers, M.M., 2011. Intensive nitrogen loss over the Omani Shelf due to anammox coupled with dissimilatory nitrite reduction to ammonium. ISME J. 5 (10), 1660–1670. https://doi.org/10.1038/ismej.2011.44.

Kalvelage, T., Lavik, G., Lam, P., Contreras, S., Arteaga, L., Löscher, C.R., Oschlies, A., Paulmier, A., Stramma, L., Kuypers, M.M.M., 2013. Nitrogen cycling driven by organic matter export in the South Pacific oxygen minimum zone. Nat. Geosci. 6 (3), 228–234. https://doi.org/10.1038/ngeo1739.

Koike, I., Hattori, A., 1978. Denitrification and ammonia formation in anaerobic coastal sediments. Appl. Environ. Microbiol. 35 (2), 278–282.

Koop-Jakobsen, K., Giblin, A.E., 2010. The effect of increased nitrate loading on nitrate reduction via denitrification and DNRA in salt marsh sediments. Limnol. Oceanogr. 55 (2), 789–802. https://doi.org/10.4319/lo.2010.55.2.0789.

Kulp, T.R., Han, S., Saltikov, C.W., Lanoil, B.D., Zargar, K., Oremland, R.S., 2007. Effects of imposed salinity gradients on dissimilatory arsenate reduction, sulfate reduction, and other microbial processes in sediments from two California Soda Lakes. Appl. Environ. Microbiol. 73 (16), 5130. https://doi.org/10.1128/AEM.00771-07.

Kuypers, M.M.M., Marchant, H.K., Kartal, B., 2018. The microbial nitrogen-cycling network. Nat. Rev. Microbiol. 16 (5), 263–276. https://doi.org/10.1038/nrmicro.2018.9.

Lachouani, P., Frank, A.H., Wanek, W., 2010. A suite of sensitive chemical methods to determine the δ15N of ammonium, nitrate and total dissolved N in soil extracts. Rapid Commun. Mass Spectrom. 24 (24), 3615–3623. https://doi.org/10.1002/rcm.4798.

Liao, T., Wang, R., Zheng, X., Sun, Y., Butterbach-Bahl, K., Chen, N., 2013. Automated online measurement of N2, N2O, NO, CO2, and CH4 emissions based on a gas-flow-soil-core technique. Chemosphere 93 (11), 2848–2853. https://doi.org/10.1016/j.chemosphere.2013.07.001.

Liengaard, L., Figueiredo, V., Markfoged, R., Revsbech, N.P., Nielsen, L.P., Prast, A.E., Kühl, M., 2014. Hot moments of N2O transformation and emission in tropical soils from the Pantanal and the Amazon (Brazil). Soil Biol. Biochem. 75, 26–36. https://doi.org/10.1016/j.soilbio.2014.03.015.

Lipsewers, Y.A., Hopmans, E.C., Meysman, F.J.R., Sinninghe Damsté, J.S., Villanueva, L., 2016. Abundance and diversity of denitrifying and anammox bacteria in seasonally hypoxic and sulfidic sediments of the saline Lake Grevelingen. Front. Microbiol. 7, 1661. https://doi.org/10.3389/fmicb.2016.01661.

Liu, W., Wang, Z., Zhang, Q., Cheng, X., Lu, J., Liu, G., 2015. Sediment denitrification and nitrous oxide production in Chinese plateau lakes with varying watershed land uses. Biogeochemistry 123 (3), 379–390. https://doi.org/10.1007/s10533-015-0072-9.

Mallin, M.A., Johnson, V.L., Ensign, S.H., MacPherson, T.A., 2006. Factors contributing to hypoxia in rivers, lakes, and streams. Limnol. Oceanogr. 51 (1). https://doi.org/10.4319/lo.2006.51.1_part_2.0690.

Marchant, H.K., Holtappels, M., Lavik, G., Ahmerkamp, S., Winter, C., Kuypers, M.M.M., 2016. Coupled nitrification–denitrification leads to extensive N loss in subtidal permeable sediments. Limnol. Oceanogr. 61 (3), 1033–1048. https://doi.org/10.1002/lno.10271.

McCrackin, M.L., Elser, J.J., 2010. Atmospheric nitrogen deposition influences denitrification and nitrous oxide production in lakes. Ecology 91 (2), 528–539. https://doi.org/10.1890/08-2210.1.

Minjeaud, L., Michotey, V.D., Garcia, N., Bonin, P.C., 2009. Seasonal variation in di-nitrogen fluxes and associated processes (denitrification, anammox and nitrogen fixation) in sediment subject to shellfish farming influences. Aquat. Sci. 71 (4), 425–435. https://doi.org/10.1007/s00027-009-0100-8.

Mulvaney, R.L., Khan, S.A., Stevens, W.B., Mulvaney, C.S., 1997. Improved diffusion methods for determination of inorganic nitrogen in soil extracts and water. Biol. Fertil. Soils 24 (4), 413–420. https://doi.org/10.1007/s003740050266.

Nelson, D.W., Sommers, L.E., 2018. Total carbon, organic carbon, and organic matter. Methods of Soil Analysis. John Wiley & Sons, Ltd., pp. 961–1010.

Nielsen, L.P., 1992. Denitrification in sediment determined from nitrogen isotope pairing. FEMS Microbiol. Lett. 86 (4), 357–362. https://doi.org/10.1111/j.1574-6968.1992.tb04828.x.

Nowicki, B.L., 1994. The effect of temperature, oxygen, salinity, and nutrient enrichment on estuarine denitrification rates measured with a modified nitrogen gas flux technique. Estuar. Coast. Shelf Sci. 38 (2), 137–156. https://doi.org/10.1006/ecss.1994.1009.

Orellana, L.H., Rodriguez-R, L.M., Higgins, S., Chee-Sanford, J.C., Sanford, R.A., Ritalahti, K.M., Löffler, F.E., Konstantinidis, K.T., 2014. Detecting nitrous oxide reductase (nosZ) genes in soil metagenomes: method development and implications for the nitrogen cycle. MBio 5 (3). https://doi.org/10.1128/mBio.01193-14 e01193-14.

Prisu, J.C., Downes, M.T., McKay, C.P., 1996. Extreme supersaturation of nitrous oxide in a poorly ventilated Antarctic lake. Limnol. Oceanogr. 41 (7), 1544–1551. https://doi.org/10.4319/lo.1996.41.7.1544.

Prommer, J., Wanek, W., Hofmann, F., Trojan, D., Offre, P., Urich, T., Schleper, C., Sassmann, S., Kitzler, B., Soja, G., Hood-Nowotny, R.C., 2014. Biochar decelerates soil organic nitrogen cycling but stimulates soil nitrification in a temperate arable field trial. PLoS One 9 (1), e86388. https://doi.org/10.1371/journal.pone.0086388.

Ravishankara, A.R., Daniel, J.S., Portmann, R.W., 2009. Nitrous oxide (N2O): the dominant ozone-depleting substance emitted in the 21st century. Science 326 (5949), 123–125. https://doi.org/10.1126/science.1176985.

Risgaard-Petersen, N., Rysgaard, S., Nielsen, L.P., Revsbech, N.P., 1994. Diurnal variation of denitrification and nitrification in sediments colonized by benthic microphytes. Limnol. Oceanogr. 39 (3), 573–579. https://doi.org/10.4319/lo.1994.39.3.0573.

Risgaard-Petersen, N., Nielsen, L.P., Rysgaard, S., Dalsgaard, T., Meyer, R.L., 2003. Application of the isotope pairing technique in sediments where anammox and denitrification coexist. Limnol. Oceanogr. Methods 1 (1), 63–73. https://doi.org/10.4319/lom.2003.1.63.

Risgaard-Petersen, N., Meyer, R.L., Schmid, M., Jetten, M.S.M., Enrich-Prast, A., Rysgaard, S., Reysbech, N.P., 2004. Anaerobic ammonium oxidation in an estuarine sediment. Aquat. Microb. Ecol. 36 (3), 293–304. https://doi.org/10.3354/ame036293.

Robarts, R.D., Waiser, M.J., Arts, M.T., Evans, M.S., 2005. Seasonal and diel changes of dissolved oxygen in a hypertrophic prairie lake. Lakes Reserv. Res. Manag. 10, 167–177. https://doi.org/10.1111/j.1440-1770.2005.00273.x.

Robertson, E.K., Bartoli, M., Brüchert, V., Dalsgaard, T., Hall, P.O.J., Hellemann, D., Hietanen, S., Zilius, M., Conley, D.J., 2019. Application of the isotope pairing technique in sediments: use, challenges, and new directions. Limnol. Oceanogr. Methods 17 (2), 112–136. https://doi.org/10.1002/lom3.10303.

Roland, F.A.E., Darchambeau, F., Borges, A.V., Morana, C., De Brabandere, L., Thamdrup, B., Crowe, S.A., 2018. Denitrification, anaerobic ammonium oxidation, and dissimilatory nitrate reduction to ammonium in an East African Great Lake (Lake Kivu). Limnol. Oceanogr. 63 (2), 687–701. https://doi.org/10.1002/lno.10660.

Salahudeen, J.H., Reshmi, R.R., Anoop Krishnan, K., Ragi, M.S., Vincent, S.G.T., 2018. Denitrification rates in estuarine sediments of ashtamudi, Kerala, India. 190 (6), 323. https://doi.org/10.1007/s10661-018-6698-z.

Salk, K.R., Erler, D.V., Eyre, B.D., Carlson-Perret, N., Ostrom, N.E., 2017. Unexpectedly high degree of anammox and DNRA in seagrass sediments: description and application of a revised isotope pairing technique. Geochim. Cosmochim. Acta 211, 64–78. https://doi.org/10.1016/j.gca.2017.05.012.

Schmidt, I., Sliekers, O., Schmid, M., Cirpus, I., Strous, M., Bock, E., Kuenen, J.G., Jetten, M.S.M., 2002. Aerobic and anaerobic ammonia oxidizing bacteria – competitors or natural partners? FEMS Microbiol. Ecol. 39 (3), 175–181. https://doi.org/10.1111/j.1574-6941.2002.tb00920.x.

Schubert, C.J., Durisch-Kaiser, E., Wehrli, B., Thamdrup, B., Lam, P., Kuypers, M.M.M., 2006. Anaerobic ammonium oxidation in a tropical freshwater system (Lake Tanganyika). Environ. Microbiol. 8 (10), 1857–1863. https://doi.org/10.1111/j.1462-2920.2006.01074.x.

Shapovalova, A.A., Khijniak, T.V., Tourova, T.P., Muyzer, G., Sorokin, D.Y., 2008. Heterotrophic denitrification at extremely high salt and pH by haloalkaliphilic gammaproteobacteria from hypersaline soda lakes. Extremophiles 12 (5), 619–625. https://doi.org/10.1007/s00792-008-0166-6.

Smith, L.K., Voytek, M.A., Böhlke, J.K., Harvey, J.W., 2006. Denitrification in nitrate-rich streams: application of N2: ar and 15N-tracer methods in intact cores. Ecol. Appl. 16 (6), 2191–2207. https://doi.org/10.1890/1051-0761(2006)016[2191:DINSAO]2.0.CO;2.

Song, G.D., Liu, S.M., Marchant, H., Kuypers, M.M.M., Lavik, G., 2013. Anammox, denitrification and dissimilatory nitrate reduction to ammonium in the East China Sea sediment. Biogeosciences 10 (11), 6851–6864. https://doi.org/10.5194/bg-10-6851-2013.

Song, G.D., Liu, S.M., Kuypers, M.M.M., Lavik, G., 2016. Application of the isotope pairing technique in sediments where anammox, denitrification, and dissimilatory nitrate reduction to ammonium coexist. Limnol. Oceanogr. Methods 14 (12), 801–815. https://doi.org/10.1002/lom3.10127.

Sørensen, P., Jensen, E.S., 1991. Sequential diffusion of ammonium and nitrate from soil extracts to a polytetrafluoroethylene trap for 15N determination. Anal. Chim. Acta 252 (1), 201–203. https://doi.org/10.1016/0003-2670(91)87215-S.

Spalding, R.F., Exner, M.E., 1993. Occurrence of nitrate in groundwater—a review. J. Environ. Qual. 22, 392–402. https://doi.org/10.2134/jeq1993.00472425002200030002x.

Stevens, R.J., Laughlin, R.J., Atkins, G.J., Prosser, S.J., 1993. Automated determination of Nitrogen-15-labeled dinitrogen and nitrous oxide by mass spectrometry. Soil Sci. Soc. Am. J. 57 (4), 981–988. https://doi.org/10.2136/sssaj1993.03615995005700040017x.

Tan, E., Zou, W., Jiang, X., Wan, X., Hsu, T.-C., Zheng, Z., Chen, L., Xu, M., Dai, M., Kao, S., 2019. Organic matter decomposition sustains sedimentary nitrogen loss in the Pearl River estuary, China. Sci. Total Environ. 648, 508–517. https://doi.org/10.1016/j.scitotenv.2018.08.109.

Thamdrup, B., Dalsgaard, T., 2002. Production of N2 through anaerobic ammonium oxidation coupled to nitrate reduction in marine sediments. Appl. Environ. Microbiol. 68 (3), 1312. https://doi.org/10.1128/AEM.68.3.1312-1318.2002.

Tobias, C.R., Anderson, I.C., Canuel, E.A., Macko, S.A., 2001. Nitrogen cycling through a fringing marsh-aquifer ecotone. Mar. Ecol. Prog. Ser. 210, 25–39.

Trimmer, M., Engström, P., 2011. Distribution, activity, and ecology of anammox bacteria in aquatic environments. Available from: Nitrification, American Society of Microbiology . https://www.asmscience.org/content/book/10.1128/9781555817145.ch09.

Trimmer, M., Nicholls, J.C., Deflandre, B., 2003. Anaerobic ammonium oxidation measured in sediments along the Thames Estuary, United Kingdom, Appl. Environ. Microbiol. 69 (11), 6447. https://doi.org/10.1128/AEM.69.11.6447-6454.2003.

Trimmer, M., Risgaard-Petersen, N., Nicholls, J.C., Engström, P., 2006. Direct measurement of anaerobic ammonium oxidation (anammox) and denitrification in intact sediment cores. Mar. Ecol. Prog. Ser. 326, 37–47. https://doi.org/10.3354/meps326037.

Trogler, W.C., 1999. Physical properties and mechanisms of formation of nitrous oxide. Coord. Chem. Rev. 187 (1), 303–327. https://doi.org/10.1016/S0010-8545(98)00254-9.

Utsumi, M., Nojiri, Y., Nakamura, T., Nozawa, T., Otsuki, A., Seki, H., 1998. Oxidation of dissolved methane in a eutrophic, shallow lake: Lake Kasumigaura, Japan. 3. https://doi.org/10.4319/lo.1998.43.3.0471.

Valiente, N., Carrey, R., Otero, N., Gutiérrez-Villanueva, M.A., Soler, A., Sanz, D., Castaño, S., Gómez-Alday, J.J., 2017. Tracing sulfate recycling in the hypersaline Pétrola Lake (SE Spain): a combined isotopic and microbiological approach. Chem. Geol. 473, 74–89. https://doi.org/10.1016/j.chemgeo.2017.10.024.

Valiente, N., Carrey, R., Otero, N., Soler, A., Sanz, D., Muñoz-Martín, A., Jirsa, F., Wanek, W., Gómez-Alday, J.J., 2018. A multi-isotopic approach to investigate the influence of land use on nitrate removal in a highly saline lake-aquifer system. Sci. Total Environ. 631–632, 649–659. https://doi.org/10.1016/j.scitotenv.2018.03.059.

van de Graaf, A.A., Mulder, A., de Bruijn, P., Jetten, M.S., Robertson, L.A., Kuenen, J.G., 1995. (1995) anaerobic oxidation of ammonium is a biologically mediated process. Appl. Environ. Microbiol. 61 (4), 1246.

van den Berg, E.M., Rombouts, J.L., Kuenen, J.G., Kleerebezem, R., van Loosdrecht, M.C., 2017a. Role of nitrite in the competition between denitrification and DNRA in a chemostat enrichment culture. AMB Express 7 (1), 1–7. https://doi.org/10.1186/s13568-017-0398-x.

van den Berg, E.M., Elisário, M.P., Kuenen, J.G., Kleerebezem, R., van Loosdrecht, M.C., 2017b. Fermentative bacteriainfluence the competition between denitrifiers and DNRA bacteria. Front. Microbiol. 8, 1684. https://doi.org/10.3389/fmicb.2017.01684.

van der Wielen, P.W.J.J., Bolhuis, H., Borin, S., Daffonchio, D., Corselli, C., Giuliano, L., D'Auria, G., de Lange, G.J., Huebner, A., Varnavas, S.P., Thomson, J., Tamburini, C., Marty, D., McGenity, T.J., Timmis, K.N., 2005. The enigma of prokaryoticlife in

deephypersalineanoxicbasins. Science 307 (5706), 121. https://doi.org/10.1126/science.1103569.

Vitousek, P.M., Aber, J.D., Howarth, R.W., Likens, G.E., Matson, P.A., Schindler, D.W., Schlesinger, W.H., Tilman, D.G., 1997. Human alteration of the global nitrogen cycle: sources and consequences. Ecol. Appl. 7 (3), 737–750. https://doi.org/10.1890/1051-0761(1997)007[0737:HAOTGN]2.0.CO;2.

Wang, R., Willibald, G., Feng, Q., Zheng, X., Liao, T., Brüggemann, N., Butterbach-Bahl, K., 2011. Measurement of N2, N2O, NO, and CO2 emissions from soil with the gas-flow-soil-core technique. Environ. Sci. Technol. 45 (14), 6066–6072. https://doi.org/10.1021/es1036578.

Wang, S., Hong, Y., Wu, J., Xu, X.-R., Bin, L., Pan, Y., Guan, F., Wen, J., 2015. Comparative analysis of two 16S rRNA gene-based PCR primer sets provides insight into the diversity distribution patterns of anammox bacteria in different environments. Appl. Microbiol. Biotechnol. 99 (19), 8163–8176. https://doi.org/10.1007/s00253-015-6814-8.

Weiss, R.F., 1970. The solubility of nitrogen, oxygen and argon in water and seawater. Deep-Sea Res. Oceanogr. Abstr.. 17 (4), 721–735. https://doi.org/10.1016/0011-7471(70)90037-9.

Weiss, R.F., Craig, H., 1973. Precise shipboard determination of dissolved nitrogen, oxygen, argon, and total inorganic carbon by gas chromatography. Deep-Sea Res. Oceanogr. Abstr. 20 (4), 291–303. https://doi.org/10.1016/0011-7471(73)90054-5.

Weiss, R.F., Price, B.A., 1980. Nitrous oxide solubility in water and seawater. Mar. Chem. 8 (4), 347–359. https://doi.org/10.1016/0304-4203(80)90024-9.

Welti, N., Bondar-Kunze, E., Mair, M., Bonin, P., Wanek, W., Pinay, G., Hein, T., 2012. Mimicking floodplain reconnection and disconnection using 15N mesocosm incubations. Biogeosciences 9 (11), 4263–4278. https://doi.org/10.5194/bg-9-4263-2012.

Wenk, C.B., Blees, J., Zopfi, J., Veronesi, M., Bourbonnais, A., Schubert, C.J., Niemann, H., Lehmann, M.F., 2013. Anaerobic ammonium oxidation (anammox) bacteria and sulfide-dependent denitrifiers coexist in the water column of a meromictic south-alpine lake. Limnol. Oceanogr. 58 (1), 1–12. https://doi.org/10.4319/lo.2013.58.1.0001.

Wenk, C.B., Zopfi, J., Gardner, W.S., McCarthy, M.J., Niemann, H., Veronesi, M., Lehmann, M.F., 2014. Partitioning between benthic and pelagic nitrate reduction in the Lake Lugano south basin. Limnol. Oceanogr. 59 (4), 1421–1433. https://doi.org/10.4319/lo.2014.59.4.1421.

Wickramasinghe, K.N., Taljbudeen, O., Witty, J.F., 1978. A gas flow-through system for studying denitrification in soil. J. Soil Sci. 29 (4), 527–536. https://doi.org/10.1111/j.1365-2389.1978.tb00801.x.

Williams, W.D., 2002. Environmental threats to salt lakes and the likely status of inland saline ecosystems in 2025. Environ. Conserv. 29 (2), 154–167. https://doi.org/10.1017/S0376892902000103.

Xue, Y., Yu, Z., Chen, H., Yang, J.R., Liu, M., Liu, L., Huang, B., Yang, J., 2017. Cyanobacterial bloom significantly boosts hypolimnelic anammox bacterial abundance in a subtropical stratified reservoir. FEMS Microbiol. Ecol. 93 (fix118). https://doi.org/10.1093/femsec/fix118.

Yang, J., Jiang, H., Wu, G., Hou, W., Sun, Y., Lai, Z., Dong, H., 2012. Co-occurrence of nitrite-dependent anaerobic methane oxidizing and anaerobic ammonia oxidizing bacteria in two Qinghai-Tibetan saline lakes. Front. Earth Sci. 6 (4), 383–391. https://doi.org/10.1007/s11707-012-0336-9.

Yoon, S., Nissen, S., Park, D., Sanford, R.A., Löffler, F.E., 2016. Nitrous oxide reduction kinetics distinguish bacteria harboring clade I NosZ from those harboring clade II NosZ. Appl. Environ. Microbiol. 82 (13), 3793. https://doi.org/10.1128/AEM.00409-16.

Zhao, Y., Xia, Y., Ti, C., Shan, J., Li, B., Xia, L., Yan, X., 2015. Nitrogen removal capacity of the river network in a high nitrogen loading region. Environ. Sci. Technol. 49 (3), 1427–1435. https://doi.org/10.1021/es504316b.